

Crustal Seismic Anisotropy in Southern California

Ryan Porter (*University of Arizona*), George Zandt (*University of Arizona*), Nadine McQuarrie (*Princeton University*)

Understanding lower crustal deformational processes and the related features that can be imaged by seismic waves is an important goal in active tectonics and seismology. Using data from publicly available stations, we calculated teleseismic receiver functions to measure crustal anisotropy at 38 broadband seismic stations in southern California. Results reveal a signature of pervasive seismic anisotropy located in the lower crust that is consistent with the presence of schists emplaced during Laramide flat slab subduction. Anisotropy is identified in receiver functions by the large amplitudes and small move-out of the diagnostic converted phases. Within southern California, receiver functions from numerous stations reveal patterns indicative of a basal crustal layer of hexagonal anisotropy with a dipping symmetry axis. Neighborhood algorithm searches [Frederiksen et al., 2003] for depth and thickness of the anisotropic layer and the trend and plunge of the anisotropy symmetry (slow) axis have been completed for the stations. The searches produced a wide range of results but a dominant SW-NE trend of the anisotropy symmetry axes emerged among the measurements. When the measurements were assigned to crustal blocks and restored to their pre-36 Ma locations and orientations using the reconstruction of McQuarrie and Wernicke [2005], the regional scale SW-NE trend became even more consistent (Fig. 1). This suggests that anisotropy predates Pacific-North American plate strike slip motion, though a small subset of the results can be attributed to NW-SE shearing that may be related to San Andreas transform motion (Fig 1). We interpret this dominant trend as a fossilized fabric within schists, created from a top-to-the-southwest sense of shear that existed along the length of coastal California during pre-transform, early Tertiary subduction. Comparison of receiver function common conversion point stacks to seismic models from the active LARSE experiment shows a strong correlation between the location of anisotropic layers and “bright” reflectors from Fuis et al. [2007], further affirming these results (Fig. 2).

References

- Frederiksen, A. W., H. Folsom, and G. Zandt (2003), Neighbourhood inversion of teleseismic Ps conversions for anisotropy and layer dip, *Geophys. J. Int.*, 155(1), 200-212.
- Fuis, G. S., M. D. Kohler, M. Scherwath, U. ten Brink, H. J. A. Van Avendonk, and J. M. Murphy (2007), A comparison between the transpressional plate boundaries of the South Island, New Zealand, and southern California, USA: the Alpine and San Andreas Fault systems, in *A Continental Plate Boundary: Tectonics at South Island, New Zealand*, edited by D. Okaya, T. Stern and F. Davey, pp. 307-327, American Geophysical Union.
- McQuarrie, N., and B. P. Wernicke (2005), An animated tectonic reconstruction of southwestern North America since 36 Ma *Geosphere*, 1(3), 147-172.

Acknowledgements: This work was funded by a grant from Southern California Earthquake Center and NSF EAR Earthscope Program award #0745588.

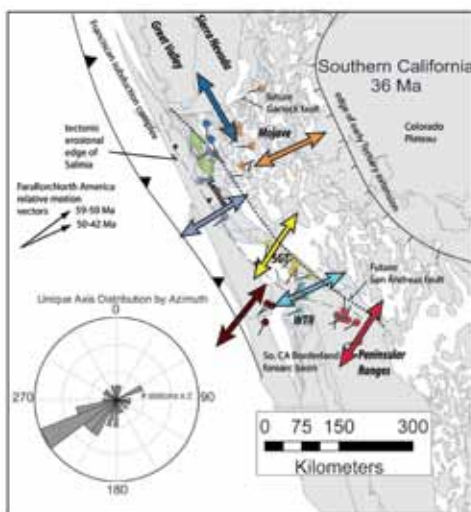


Figure 1. Map of station locations and unique anisotropy axis orientations at 36 Ma based on the reconstruction of McQuarrie and Wernicke (2005). Station color-coding corresponds to the crustal blocks. The large arrows show the best fitting block trend-lines rotated back to their orientation at 36 Ma. The rose diagram shows the number of stations with anisotropy trends within each 10° bin when rotated back to their 36 Ma orientations. Vectors show Early Tertiary Farallon-North America relative motion vectors.

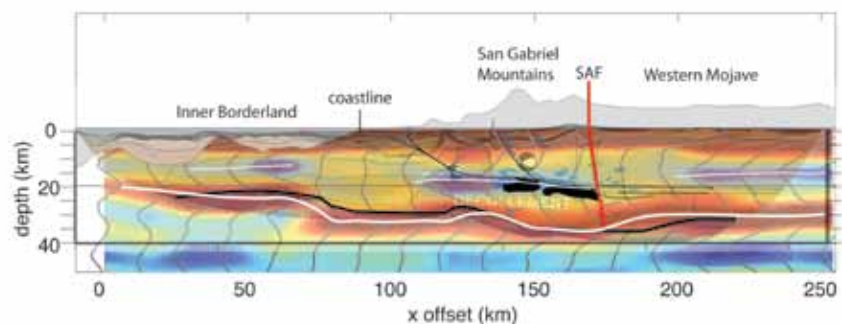


Figure 2. Common Conversion Point (CCP) cross-section for southern California, overlain with results from the LARSE project (Fuis et al., 2007) to illustrate similarities. In the RF stack, red shading corresponds to positive polarity arrivals and blue to negative. The thick white line represents the RF Moho, while the thick black line represents the LARSE Moho. Thin white lines represent structures (i.e., top of potential shear zones) seen in RFs. The thin black lines represent reflectors interpreted as a decollement in the LARSE cross-section and the thick black bodies represent the LARSE bright reflectors (Fuis et al., 2007). The thick vertical red line is the projection of the San Andreas fault.

Adjoint Tomography of the Southern California Crust

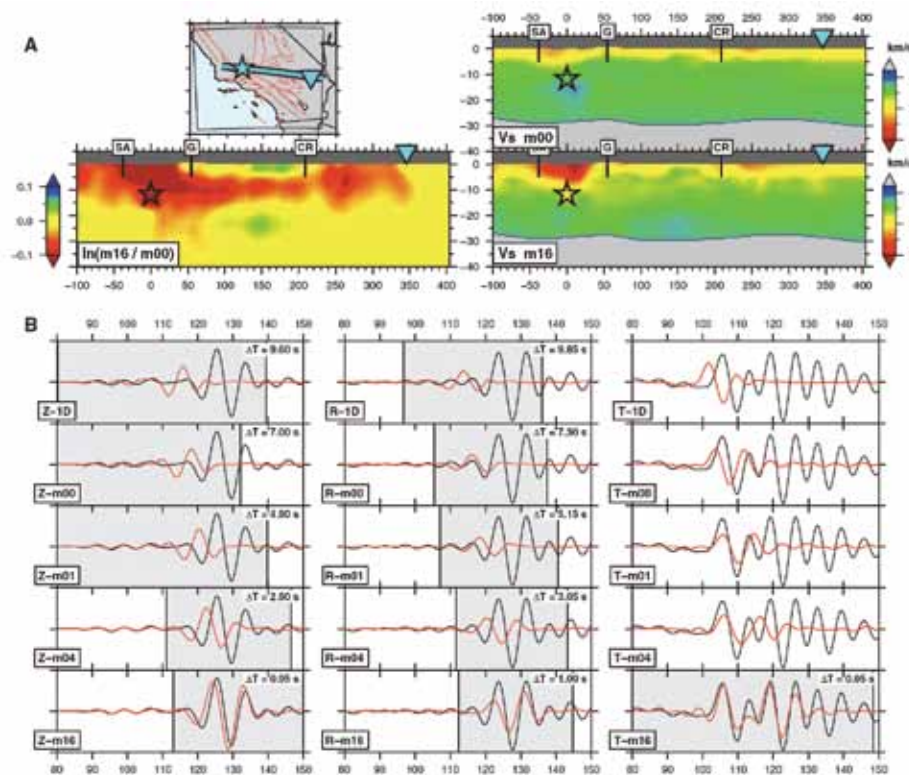
Carl Tape (Harvard University), Qinya Liu (University of Toronto), Alessia Maggi (University of Strasbourg), Jeroen Tromp (Princeton University)

We iteratively improve a 3D tomographic model of the southern California crust using numerical simulations of seismicwave propagation based on a spectral-element method (SEM) in combination with an adjoint method. The initial 3D model is provided by the Southern California Earthquake Center. The data set comprises three-component seismicwaveforms (i.e. both body and surface waves), filtered over the period range 2-30 s, from 143 local earthquakes recorded by a network of 203 stations. Time windows for measurements are automatically selected by the FLEXWIN algorithm. The misfit function in the tomographic inversion is based on frequency-dependent multitaper traveltime differences. The gradient of the misfit function and related finite-frequency sensitivity kernels for each earthquake are computed using an adjoint technique. The kernels are combined using a source subspace projection method to compute a model update at each iteration of a gradient-based minimization algorithm. The inversion involved 16 iterations, which required 6800 wavefield simulations. The new crustal model, m16, is described in terms of independent shear (V_s) and bulk-sound (V_b) wave speed variations. It exhibits strong heterogeneity, including local changes of ± 30 percent with respect to the initial 3D model. The model reveals several features that relate to geological observations, such as sedimentary basins, exhumed batholiths, and contrasting lithologies across faults. The quality of the new model is validated by quantifying waveform misfits of full-length seismograms from 91 earthquakes that were not used in the tomographic inversion. The new model provides more accurate synthetic seismograms that will benefit seismic hazard assessment.

References

- Tape, C., Liu, Q., Maggi, A., Tromp, J., 2009, Adjoint tomography of the southern California crust, *Science*, 325, 988–992.
- Tape, C., Liu, Q., Maggi, A., Tromp, J., 2010, Seismic tomography of the southern California crust based on spectral-element and adjoint methods, *Geophys. J. Int.*, 180, 433-462.
- Maggi, A., Tape, C., Chen, M., Chao, D., Tromp, J., 2009, An automated time-window selection algorithm for seismic tomography, *Geophys. J. Int.*, 178, 257–281.

Acknowledgements: Seismic waveforms were provided by the data centers listed in Table 2 (IRIS, SCEDC, NCEDC). All earthquake simulations were performed on the CITerra Dell cluster at the Division of Geological & Planetary Sciences (GPS) of the California Institute of Technology. We acknowledge support by the National Science Foundation under grant EAR-0711177. This research was supported by the Southern California Earthquake Center. SCEC is funded by NSF Cooperative Agreement EAR-0106924 and USGS Cooperative Agreement 02HQAG0008.



Iterative improvement of a three-component seismicogram. (A) Cross section of the V_s tomographic models for a path from a Mw 4.5 earthquake (star) on the White Wolf fault to station DAN (triangle) in the eastern Mojave Desert. Upper right is the initial 3D model, m00; lower right is the final 3D model, m16; and lower left is the difference between the two, $\ln(m16/m00)$. Faults labeled for reference are San Andreas (SA), Garlock (G), and Camp Rock (CR). (B) Iterative three-component seismicogram fits to data for models m00, m01, m04, and m16. Also shown are synthetic seismograms computed for a standard 1D model. Synthetic seismograms (red) and recorded seismograms (black), filtered over the period range 6 to 30 s. Left column, vertical component (Z); center column, radial component (R); right column, transverse component (T). Inset "DT" label indicates the time shift between the two windowed records that provides the maximum cross-correlation.

Nature of Crustal Terranes and the Moho in Northern Costa Rica from Receiver Function Analysis

Lepolt Linkimer (Department of Geosciences, University of Arizona), **Susan L. Beck** (Department of Geosciences, University of Arizona), **Susan Y. Schwartz** (Department of Earth and Planetary Sciences, University of California), **George Zandt** (Department of Geosciences, University of Arizona), **Vadim Levin** (Department of Earth and Planetary Sciences, Rutgers University)

The Central American subduction zone in northern Costa Rica shows along-strike variations in both the incoming and overriding plates. By analyzing the subducting oceanic Moho (M1) and the upper plate Moho (M2) with receiver functions, we investigate the variability in the hydration state of the subducting Cocos Plate and the nature of crustal terranes within the overriding Caribbean Plate. We calculate high-quality P- and PP- wave receiver functions using broadband data of the Global Seismology Network, Geoscope Project, and the CRSEIZE, Pocosol, and Corisubmod experiments. In addition, we estimate the depth (H) and vertically averaged V_p/V_s (k) to Moho and present a sensitivity study to explore the effects of a dipping interface on receiver functions and the H and k estimates. Our results are consistent with a drier oceanic mantle subducting beneath the southernmost part of the Nicoya Peninsula, as compared to a serpentinized oceanic mantle subducting beneath the northern part. In the Caribbean Plate, we describe the nature of the Mesquito, Nicoya, and Chorotega terranes by integrating new and published V_p/V_s estimates. Both the Nicoya and Chorotega terranes display high V_p/V_s (1.80-1.92) consistent with their oceanic character. In contrast, the oceanic Mesquito Terrane mostly displays lower V_p/V_s (1.62-1.80) more compatible with continental crust, which may indicate that subduction zone magmatism is modifying the crust to display continental character (see Figure). Our estimates show that the deepest M2 (~42 km) is observed in the volcanic arc region whereas the shallowest M2 (~27-33 km) is observed in parts of the fore-arc and back-arc regions.

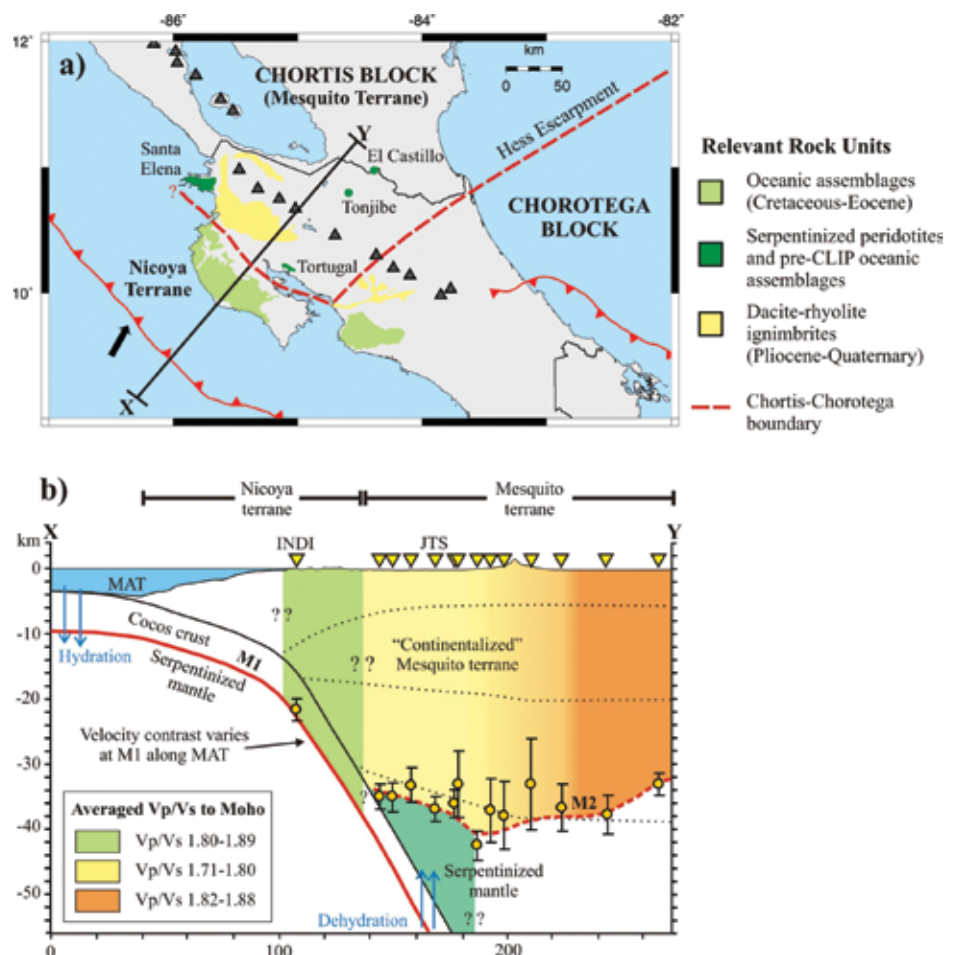
References

DeShon, H. R., and S. Y. Schwartz (2004), Evidence for serpentinization of the forearc mantle wedge along the Nicoya Peninsula, Costa Rica, *Geophys. Res. Lett.*, 31, L21611.

MacKenzie, L., G. A. Abers, K. M. Fischer, E. M. Syracuse, J. M. Protti, V. Gonzalez, and W. Strauch (2008), Crustal structure along the southern Central American volcanic front, *Geochem. Geophys. Geosyst.*, 9, Q08S09.

Sallarès, V., J. J. Dañobeitia, and E. R. Flueh (2001), Lithospheric structure of the Costa Rican Isthmus: Effects of subduction zone magmatism on an oceanic plateau, *J. Geophys. Res.*, 106(B1), 621-643.

Acknowledgements: Data from stations JTS, HDC, and CRSEIZE (in part) were obtained from the Data Management Center via IRIS. Thanks to S. Husen and V. Maurer for making the CORISUBMOD data available. Partial funding was provided by NSF grants EAR0510966 (S. Beck and G. Zandt) and EAR0506463 (S. Schwartz).



Generalized interpretation of terrane boundaries at surface (a) and along the X-Y cross-section (b) integrating results from this study, DeShon and Schwartz [2004], MacKenzie et al. [2008], and Sallarès et al. [2001].

Crustal Structure of the High Lava Plains of Oregon: A Large Controlled-Source Experiment

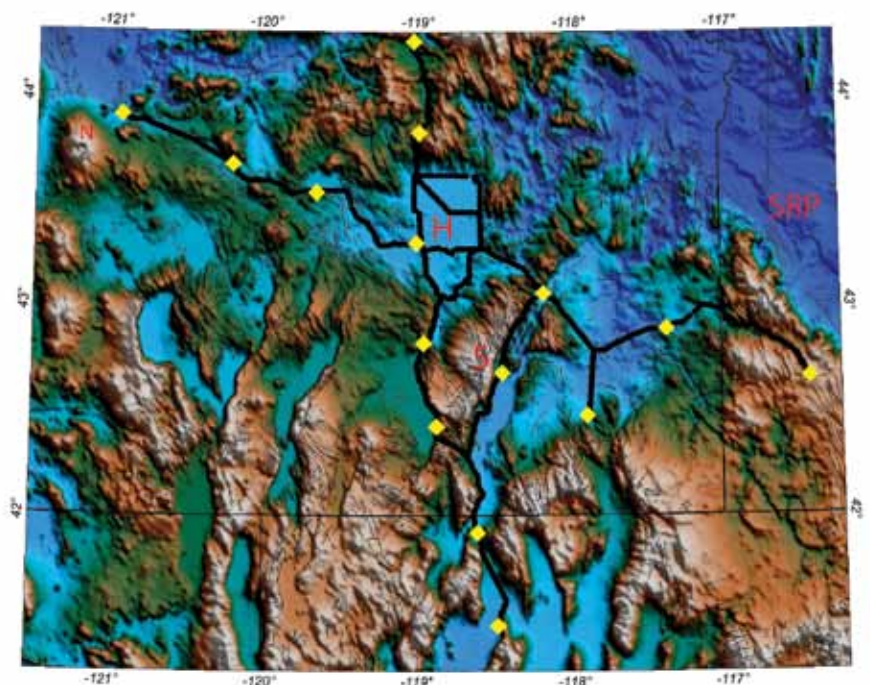
Catherine Cox (*University of Oklahoma*), Randy Keller (*University of Oklahoma*)

The High Lava Plains (HLP) of eastern Oregon and adjacent parts of Idaho and Nevada were the target of a very large controlled-source seismic experiment in early September 2008. This survey was designed to image the crust and upper mantle with the purpose of understanding the tectonics and mechanisms that drive the intraplate volcanism of the High Lava Plains and how this volcanism is related to the Cascade subduction zone and the Basin and Range province. This survey proved successful thanks to the 67 scientists, students, and volunteers deployed 2612 Texan short-period seismic recorders and 120 RT-130 recorders from the PASSCAL and EarthScope instrument pools, and fired 15 seismic sources spaced across the High Lava Plains (HLP) region. This was the largest number of instruments deployed in an on-land controlled-source seismic experiment on a crustal scale. This army of helpers included 42 students from 12 different universities, mainly the University of Oklahoma, Stanford, Oregon State, Arizona State, MIT, Miami-Ohio, University of Texas at Dallas, and Rhode Island, as well as a team from the Carnegie Institution of Washington. These deployers were ably assisted by 6 staff members from the PASSCAL/EarthScope Instrument Center. This deployment also took advantage of the >100 seismometers in the HLP broadband array whose deployment over the three years was led by Carnegie Institution of Washington and Arizona State University. The University of Oregon, Michigan Tech, and the U. S. Geological Survey also deployed an array in the Newberry volcano area to record earthquakes and the seismic sources. Together, these efforts are providing a deep and three-dimensional image of the structure of this region.

New instrumentation built by the PASSCAL Instrument Center staff made it possible to carry out 3C recording using three Texan single-channel instruments at a site to study detailed crustal structure and anisotropy across the towering Steens Mountain region. The seismometers were located to provide high-resolution images of the mantle and crust directly beneath the path of volcanism that dotted the High Lava Plains during the past 16 Ma. In addition to the seismic component, the overarching project, funded by the National Science Foundation's Continental Dynamics program, includes field geologists, petrologists, and geodynamicists interested in resolving the origin of the sudden massive outpouring of basalt volcanism 16 million years ago and the puzzling trend of age-progressive rhyolite domes that reaches west toward Newberry volcano, the youngest complex in the trend. Our results show that: 1) the crust thickens east of Steens Mountain near the 0.706 Sr isotope line; 2) Basin and Range structures extend well north of their physiographic expression; and 3) HLP lower crust has relatively high velocity suggesting underplating.

Acknowledgements: This study was supported by the Continental Dynamics Program of the National Foundation (Award EAR-0641515)

Index map of the High Lava Plains controlled-source experiment. Yellow diamonds indicate shot points; black lines indicate the main instrument deployment. N-Newberry Volcano. H-Harney Basin. S-Steens Mountain. SRP-Snake River Plain.



Shear Velocity Images of the Cascadia ETS Source Region

Josh A. Calkins (*Lamont-Doherty Earth Observatory*), Geoffrey A. Abers (*Lamont-Doherty Earth Observatory*), Göran Ekström (*Lamont-Doherty Earth Observatory*), Kenneth C. Creager (*University of Washington*), Stéphane Rondenay (*Massachusetts Institute of Technology*)

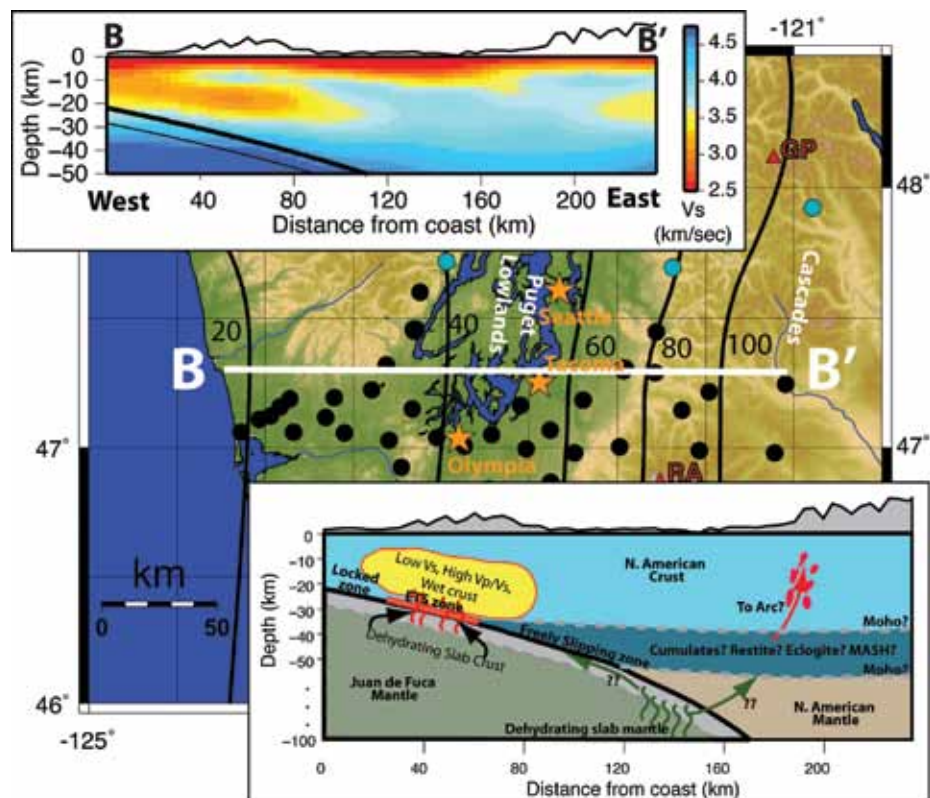
High-resolution 3D shear velocity (V_s) images of the western Washington lithosphere reveal structural segmentation above and below the plate interface correlating with transient deformation patterns. Using a spectral technique [Ekström et al, 2009], we extracted phase velocities from cross-correlated ambient noise recorded by the densely spaced “CAFE” Earthscope FlexArray. The spectral approach resolves shear velocities at station offsets less than 1 wavelength, significantly shorter than typically obtained by standard group-velocity approaches, increasing the number of useable paths and resolution. Tomographic images clearly illuminate the high V_s (>4.5 km/sec) subducting slab mantle. The most prominent anomaly is a zone of low V_s (3.0-3.3 km/sec) in the mid to lower continental crust, directly above the portion of the slab expected to be undergoing dehydration reactions. This low velocity zone (LVZ), which is most pronounced beneath the Olympic Peninsula, covers an area both spatially coincident with and updip of the region of most intense episodic tremor and slip (ETS). The low V_s and comparison with published P-wave velocity models indicate that V_p/V_s ratios in this region are greater than 1.9, suggesting a fluid rich lower crust. The LVZ disappears southward, near 47° N, coincident with sharp decreases in intraslab seismicity and ETS activity as well as structural changes in the slab. The spatial coincidence of these features suggests that long-term fluid-fluxing of the overriding plate via dewatering of a persistently hydrated patch of the Juan de Fuca slab may partially control slip on the plate interface and impact the rheology of the overriding continental crust.

References

- Abers G.A., L.S. Mackenzie, S.Rondenay, Z. Zhang, A.G. Wech, and K.C. Creager, 2009. Imaging the source region of Cascadia tremor and intermediated-depth earthquakes. *Geology*, 37, 1119-1122.
- Calkins, J.A., G.A. Abers, G. Ekstrom, K.C. Creager, and S. Rondenay. Shallow structure of the Cascadia subduction zone beneath western Washington from spectral ambient noise correlation. Submitted to *J. Geophys. Res.*, 2010.
- Ekström, G., G. A. Abers, and S. C. Webb, 2009. Determination of surface-wave phase velocities across USArray from noise and Aki’s spectral formulation. *Geophys. Res. Lett.*, 36, L18301.

Acknowledgements: This work was funded by the National Science Foundation grant EAR-0544847.

Results and interpretation of shear velocity imaging of Western Washington from spectral ambient noise analysis. Shaded relief map in the background shows PASSCAL stations (black circles), locations of major cities and topographic features, and the depth to the subducting slab in km (black lines and numbers, from McCrory et al, 2004). Upper panel shows shear velocity profile along line B-B’, highlighting the low V_s zone in the North American plate directly above the portion of the subducting Juan de Fuca slab (thick black line, after Abers et al, 2009) expected to be undergoing dehydration reactions. Lower right panel is a cartoon illustrating the main features of the V_s model near the center of the CAFE array and possible interpretations.



Controlled Source Seismic Experiments in Northern China

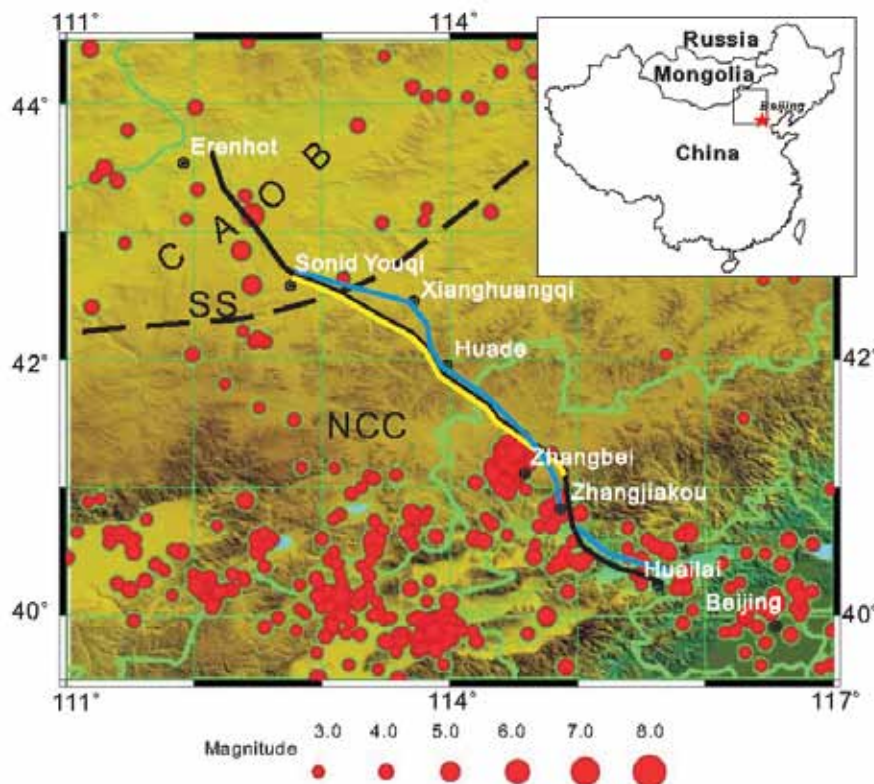
Randy Keller (*University of Oklahoma*), Gao Rui (*Chinese Academy of Geological Sciences*)

SinoProbe is China's ambitious national joint earth science research project that was established to develop a comprehensive understanding of the deep interior beneath the Chinese continent. As one of the eight major programs within SinoProbe, SinoProbe-02 initiated a large-scale controlled-source seismic experiment in North China under the leadership of the Chinese Academy of Geological Sciences (CAGS) of the Ministry of Land and Resources (MLR) in cooperation with the University of Oklahoma and University of Missouri-Columbia. This experiment was conducted in December of 2009, and consisted of three coordinated seismic recording efforts along a profile that extended from near Beijing northwestward to the Mongolian border. The profile began near the eastern edge of the Western Block of the North China Precambrian craton, crossed this feature to the Solonker suture zone, and ended in the Central Asian orogenic belt (CAOB) (Fig.1).

The CAOB is one of the world's most prominent sites of formation juvenile Phanerozoic crust. In the southern segment of the CAOB, the Solonker suture zone was involved in the final closure of the paleo-Asian Ocean and amalgamation of the North China craton and Mongolian arc terranes. South of the Solonker suture zone, the zone of seismicity around the city of Zhangbei is most seismically active region in north China and includes the 19 January 1998 Zhangbei earthquake that claimed ~50 lives and caused severe damage.

The experiment employed a combination of 2-D seismic reflection imaging and refraction/wide-angle reflection methods. The seismic reflection profile used explosive sources each recorded at 600-1200 locations for 30 seconds to create a common-midpoint (CMP) stacked image. For the refraction/wide-angle reflection portion of the experiment, 8 large shots were fired and recorded in several cases to distances of 200 km. The main seismic monitoring system employed was the single-channel RefTek 125 ("Texan") recorder from the PASSCAL/UTEP instrument pool. Along the profile, 4 deployments of 300 Texan instruments were placed a ~1 km intervals (index map, sky-blue line). In addition, 120 supplementary, 3-component recording systems were deployed as part of the reflection data recording system (index map, yellow line).

Acknowledgements: The authors acknowledge China NSF grants 40830316 and the support of Sinoprobe-02. We also thank the following participants from USA: Galen Kaip, Stephen Holloway, Steven Harder, Jefferson Chang, Catherine Cox who were funded by a US NSF PIRE grant (0730154).

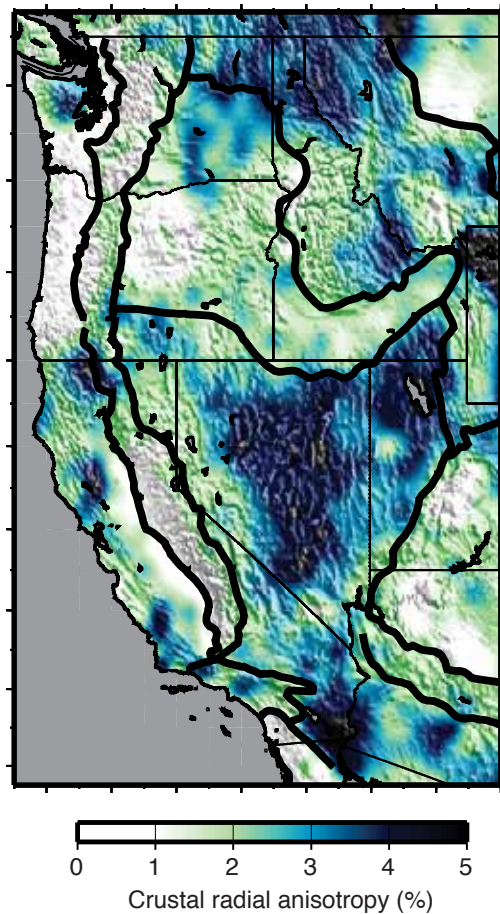


Index map of the Sinoprobe-2 reflection (black line) and refraction (yellow and blue lines) profiles. CAOB-Central Asian Orogenic Belt; SS-Solonker suture zone; NCC-North China Craton. Red circles are epicenters.

Radial Anisotropy in the Deep Crust beneath the Western US Caused by Extension

Morgan Moschetti (US Geological Survey), Michael Ritzwoller (Univ. of Colorado), Fan-Chi Lin (Univ. of Colorado), Yingjie Yang (Univ. of Colorado)

Although laboratory experiments have established that crustal rocks can be strongly anisotropic, the evidence for crustal anisotropy across large regions of the western US has not previously been documented. Surface waves can be used to identify crustal radial anisotropy (VSH \neq VSV), but the short period (< 20 s) surface wave dispersion measurements that are predominantly sensitive to crustal velocity structure are largely missing from distant earthquake signals because of scattering and attenuation. The development of noise interferometry methods now allows the measurement of surface wave dispersion at these shorter periods. Because Love and Rayleigh waves are predominantly sensitive to VSH and VSV, respectively, the simultaneous inversion of these measurements allows us to investigate the effects of crustal radial anisotropy. We invert Rayleigh and Love wave dispersion measurements from ambient noise and earthquake tomography for a radially anisotropic shear-velocity model of the crust and uppermost mantle beneath the western US (Moschetti et al., 2010a, 2010b). Where the Earth exhibits radially anisotropic properties, the effect of inverting for an isotropic model results in a characteristic data misfit termed the "Rayleigh-Love discrepancy" for which the predicted Rayleigh and Love wave speeds are faster and slower, respectively, than the observed surface wave speeds. An isotropic model results in large Rayleigh-Love discrepancies across most of the western US. We find that a model with an anisotropic uppermost mantle also results in a Rayleigh-Love discrepancy at periods that are mainly sensitive to crustal depths, but that the discrepancy is generally restricted to the Basin and Range (BR) and the Rocky Mountain BR (RMBR) provinces. The introduction of radial anisotropy in the deep crust resolves this discrepancy at all but a few, small regions in the western US. Within those geologic provinces that have experienced significant extension during the Cenozoic Era (~ 65 Ma), crustal anisotropy is often required to resolve the Rayleigh-Love discrepancy. Radial and azimuthal anisotropy in the upper mantle are generally ascribed to the alignment of olivine, and we similarly propose that the deep crustal anisotropy is caused by the alignment of anisotropic crustal minerals during crustal extension. This observation also supports the hypothesis that the response of the deep crust to crustal thinning is widespread within the extensional provinces.



Amplitude of crustal radial anisotropy in the middle and lower crust. Strong anisotropy is mainly restricted to the predominant extensional provinces (Basin and Range, Rocky Mountain Basin and Range, and Omineca Extended Belt) of the western US.

References

- Moschetti, M.P., M.H. Ritzwoller, F. Lin, Y. Yang (2010a) Seismic evidence for widespread western-US deep-crustal deformation caused by extension, *Nature*, 464, 885-889.
- Moschetti, M.P., M.H. Ritzwoller, F. Lin, Y. Yang (2010b) Crustal shear-wave velocity structure of the western US inferred from ambient seismic noise and earthquake data, *J. Geophys. Res.* (In press)
- Acknowledgements:* Research support from the National Science Foundation (NSF) (EAR-0450082 and EAR-0711526) and an NDSEG Fellowship from the American Society for Engineering Education to M.P.M. are acknowledged. The facilities of the IRIS Data Management System, and specifically the IRIS Data Management Center, were used to access the waveform and metadata required in this study.

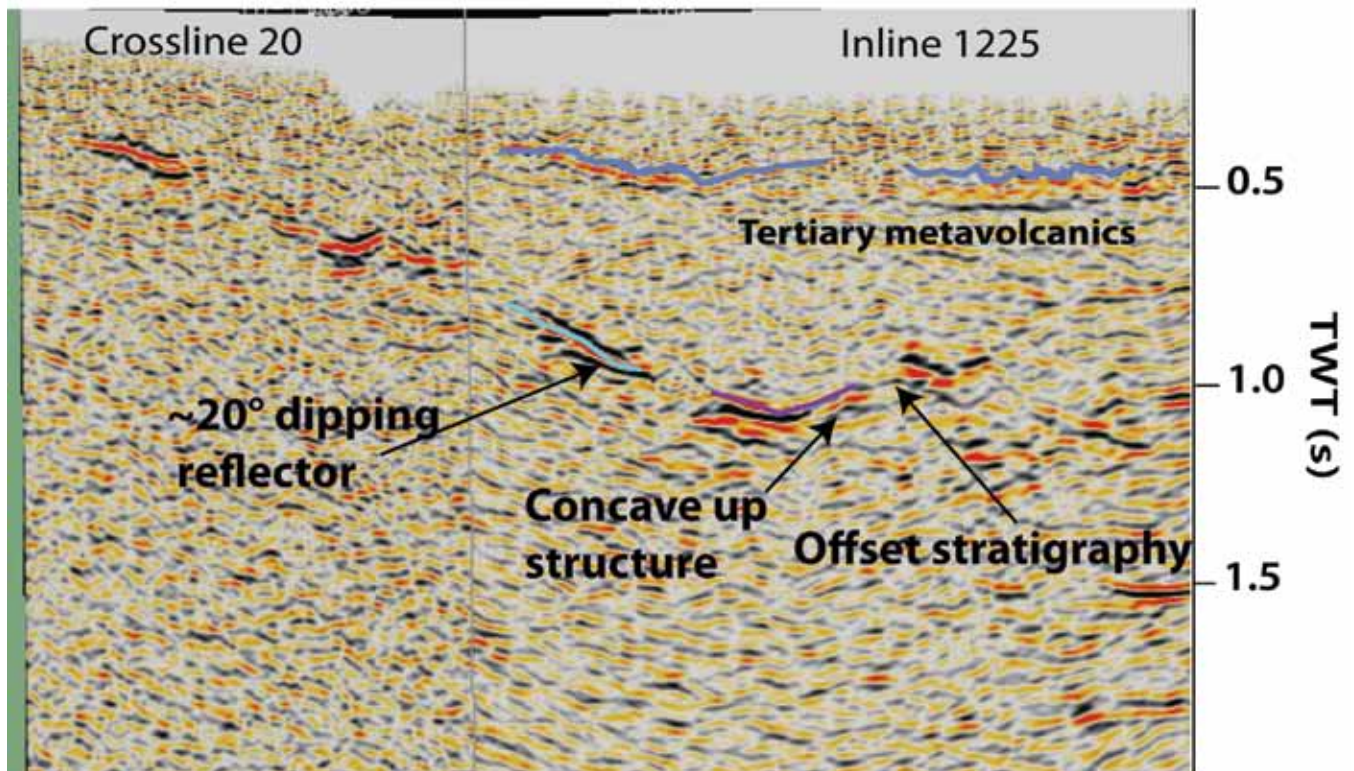
Structural Interpretations Based on a 3D Seismic Survey in Hawthorne, Nevada

Annie Kell-Hills (*Nevada Seismological Laboratory*)

Hawthorne, Nevada is located in the Walker Lake Domain of the Great Basin, a region in the western United States known for extensional tectonics and the high temperature gradients necessary for geothermal power production. Geothermal heat sources include magmatic and extensional types. The extensional type is more common for Nevada, where near-surface thermal gradients come from a thinned crust instead of from volcanism. Extensional systems often do not exhibit surface indicators such as springs or fumaroles; rather, the thermal fluids remain capped below the surface in “blind” systems requiring the need for geophysical exploration [Coolbaugh *et al.*, 2005]. Heterogeneous structure and seismic velocities common to geothermal systems create particular seismic imaging difficulties because simplifying assumptions about velocity gradients cannot be made. A 3d seismic volume collected by the Navy Geothermal Programs Office on the Hawthorne Ammunition Depot represents a rare opportunity to examine the range of geologic interpretations that can exist on seismic data in the Great Basin. Strong reflection events within the volume project to a ~20 degree dip, allowing the possibility of a low angle normal fault; while bedding offsets could be interpreted as a series of steep basin-ward step faults. Synclines in vertical sections correspond to concentric circles in horizontal sections, not only raising questions about the possibility of migration processing artifacts, but also presenting similarities to sill intrusions as seen in North Sea 3d data. This data set reveals seismic evidence for a range of structural interpretations.

References

Coolbaugh, M. F., Arehart, G. B., Faulds, J. E., & Garside, L. J. (2005). Geothermal systems in the Great Basin, western United States: Modern analogues to the roles of magmatism, structure, and regional tectonics in the formation of gold deposits . Geological Society of Nevada Symposium, 1063, 1081.



Inline and crossline sections showing strong reflections events indicating a range of structural interpretations. Inline sections clearly show 20° dipping reflectors, offset stratigraphy and synclinal events.

Assembling a Nevada 3D Velocity Model: Earthquake-Wave Propagation in the Basin & Range, and Seismic Shaking Predictions for Las Vegas

John N. Louie (University of Nevada, Reno)

The development of an open-source 3d modeling environment allows seismologists, explorationists, engineers, and students to predict wave propagation through geologically complex regions. The environment combines geologic and geotechnical data sets with gridding, modeling, and output specifications into portal packs for execution on standalone workstations, clusters, and supercomputing grids. A tutorial interface helps the user scale the grid to the facilities available, from small test runs to efforts requiring major resources. The ability to configure computations at a range of scales and model complexity is intended to promote wide use of advanced seismic modeling. Geologic models can include many basins in addition to the target urban basin, and detailed geotechnical information where available. To predict earthquake shaking in Nevada urban areas, the 3d model assembles several data sets at a wide variety of scales, from regional geologic maps to shallow shear-velocity measurements from microtremor transects having 0.3-km spacing (fig. 1). For Las Vegas the principal earthquake hazard is from the Furnace Creek fault system, capable of M7.5 events. Peak ground velocity (PGV) results from finite-difference wave modeling at 0.3 Hz show no obvious correlation between amplification and basin depth or dip of the basin floor. Animations of shaking show the expected strong trapping and long shaking durations within basins, as well as diffusion and scattering of energy between the many basins in the region. The two Furnace Creek scenarios tested, involving rupture away from and toward Las Vegas, produced unexpectedly different PGV in the city (fig. 2). Rupture directivity toward the city may amplify shaking by a factor of fifteen at some locations. Despite affecting only the very shallowest zone of models (<30 m), the Vs30 geotechnical shear-velocity shows clear correlation to 0.3-Hz PGV predictions in basins. Increasing basin thicknesses to 1.3 km correlate with increased PGV, but the basin effect at 0.3 Hz saturates for basin thicknesses greater than 1.3 km; deeper parts of the basin show variance and uncertainty of a factor of two in predicted PGV.

References

Louie, John N., 2008, Assembling a Nevada 3-d velocity model: earthquake-wave propagation in the Basin & Range, and seismic shaking predictions for Las Vegas: SEG Expanded Abstracts, 27, 2166-2170.

Acknowledgements: Research supported by the U.S. Geological Survey (USGS), Department of the Interior, under USGS award numbers 08HQGR0015 and 08HQGR0046; by Lawrence Livermore National Laboratory under LDRD Test Readiness funds; and by a Fulbright Senior Scholar award for work in New Zealand. The views and conclusions contained in this document are those of the authors and should not be interpreted as necessarily representing the official policies, either expressed or implied, of the U.S. Government. Instruments used in the field program were provided by the PASSCAL facility of the Incorporated Research Institutions for Seismology (IRIS) through the PASSCAL Instrument Center at New Mexico Tech. Data collected during this experiment will be available through the IRIS Data Management Center. The facilities of the IRIS Consortium are supported by the National Science Foundation under Cooperative Agreement EAR-0552316 and by the Department of Energy National Nuclear Security Administration.

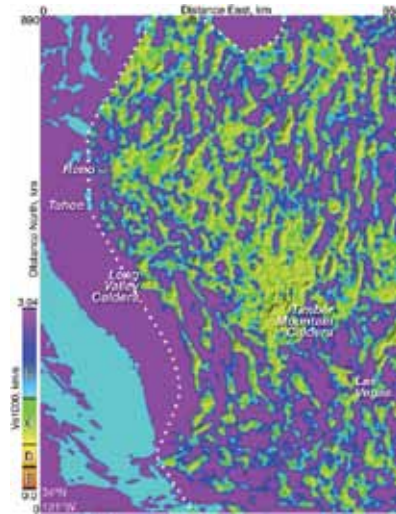


Figure 1: Map of average shear velocity from the surface to 1000 m depth assembled for the Nevada region, with part of California, on a shaded-relief basin-thickness map.

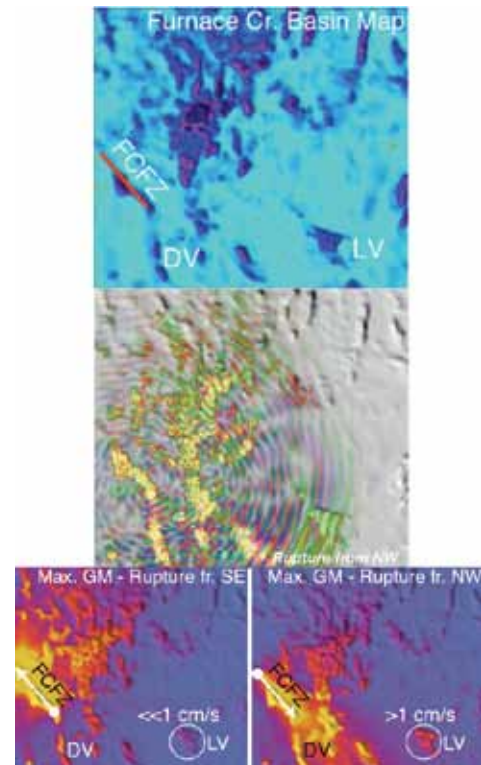


Figure 2: Maps comparing M7.5 Furnace Creek fault scenarios affecting Las Vegas. The upper image is a basin thickness map for the region of computation; middle is a snapshot map of E3D wave propagation at 0.3 Hz through the assembled model. Below are maximum ground-motion (PGV) maps, on the left for rupture away from Las Vegas, and on the right for rupture toward the city.

Optimized Velocities and Prestack Depth Migration in the Reno-Area Basin

John N. Louie (University of Nevada, Reno), Satish Pullammanappallil (Optim, Inc.), Annie Kell-Hills (University of Nevada, Reno)

We collected seismic reflection profiles in the Reno, Nevada area basin in collaboration with the USGS and nees@UTexas during June 2009. Stratigraphic horizons and vertical offsets associated with faulting appear along a 6.72 km Truckee River profile while strong, horizontally propagating body waves are seen in shot gathers from the southern 3.84 km Manzanita Lane profile (fig. 1). Reno-area basin fill overlies Miocene andesitic volcanic rocks and consists of Neogene sedimentary rocks and Quaternary outwash deposits. Using the seismic shot records, we created optimized velocity models of the Reno basin using commercial SeisOpt®@2D™ software. The refracted P-wave arrivals provide inputs for a global velocity model over the length of the profiles and to a depth proportional to the source offset distances, expected to be 150-200 m. Within this basin most of the lateral velocity heterogeneity appears within 200 m of the surface. Comparing this velocity model to stacked sections produced by the USGS added confidence to the interpretations of strong reflection boundaries seen in the seismic sections (fig. 2). Boundaries in the velocity model coincide with prominent reflection boundaries as well as with known depths of volcanic fill and other deposits, constraining their depths and velocities. The tomographic velocity sections were then used as input with the shot records to a Kirchhoff pre-stack depth migration (PSDM) imaging steeply dipping structure and further constraining current interpretations and fault/basin geometry. The PSDM resolved the cause of the horizontally propagating waves seen along Manzanita Lane as sidewall reflections from a steeply dipping fault (fig. 3).

Acknowledgements: Research supported by the U.S. Geological Survey (USGS), Department of the Interior, under USGS award numbers G09AP00051, 08HQGR0015, and 08HQGR0046. The views and conclusions contained in this document are those of the authors and should not be interpreted as necessarily representing the official policies, either expressed or implied, of the U.S. Government.

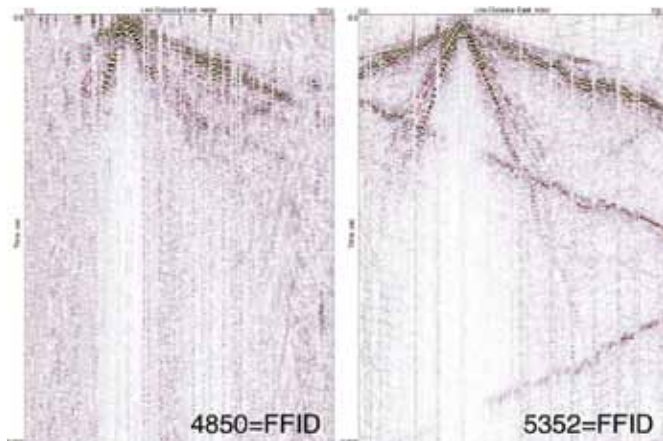


Figure 1: Two shot records from the Manzanita Lane survey, south Reno, showing strong horizontally-propagating body waves originating at surface fault traces.

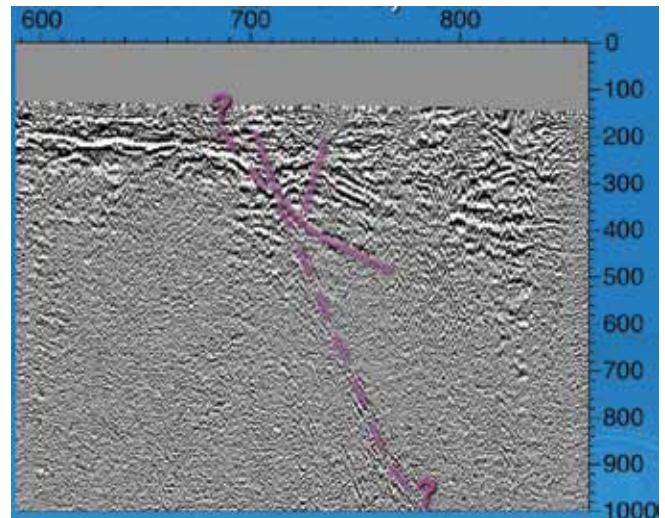


Figure 3: Portion of the depth section, 1.4 km long extending to 1000 m depth, running west (left) to east (right) along Manzanita Lane in south Reno. No vertical exaggeration- local ground surface is at 150 m depth on the vertical scale. The horizontally propagating waves image into a combination of a steeply dipping fault structure (dashed purple line) and a shallow-dipping structure (solid purple line).

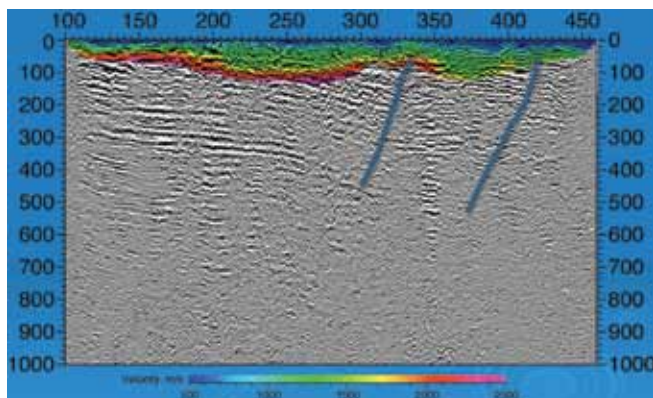


Figure 2: Depth section 2.3 km long extending to 1000 m depth, running west (left) to east (right) along the Truckee River through downtown Reno. No vertical exaggeration. Colors indicate velocities optimized from 1st-arrival picks, with Quaternary gravels (green) overlying Tertiary sands (red). The reflections are interpreted as showing two west-dipping normal faults (blue lines).

Shallow Shear-Velocity Measurements and Prediction of Earthquake Shaking in the Wellington Metropolitan Area, New Zealand

John N. Louie (*University of Nevada, Reno*)

The city of Wellington, New Zealand's capital, sits astride the Australia-Pacific plate boundary at a transition from strike slip to subduction motion. The resulting high earthquake hazard and risk motivate multiple research efforts to better understand the potential for seismic shaking. Physics-based modeling of a Landers-type M7.2 rupture on the Wellington fault, which transects the city, by Benites and Olsen [2005] showed potential for peak ground velocities as high as 1.5 m/s. Such a high hazard demands a thorough understanding of the setting, and few measurements of ground-stiffness parameters such as the average shear velocity from the surface to 30 m depth (V_{s30}) existed in Wellington prior to 1996. That year Kaiser and Louie (2006 and not yet published) made refraction microtremor measurements of V_{s30} at 46 sites in Wellington and Lower Hutt cities (fig. 1). Benites and Olsen's (2005) geotechnical model included velocities for "rock" sites that were a factor of two higher than the measurements, so we developed a revised model from the measurements. We then used the E3D physics-based modeling code of Larsen et al. [2001] to predict ground motions for a M3.2 event 8 km below the city that year, using both the original and revised models (fig. 2). The revised model is not quite as efficient at trapping wave energy in basins, as was the original model. Most of the V_{s30} measurements were made at strong-motion recording stations, so the resulting seismometer data are now better calibrated for site conditions.

References

- Benites, Rafael and Kim B. Olsen, 2005, Modeling strong ground motion in the Wellington metropolitan area, New Zealand: *Bull. Seismol. Soc. Amer.*, 95, 2180–2196.
- Kaiser, A. E., and J. N. Louie, 2006, Shear-wave velocities in Parkway basin, Wainuiomata, from refraction microtremor surface wave dispersion: GNS Science Report 2006/024, July, Lower Hutt, New Zealand, 16 pp.
- Larsen, S., Wiley, R., Roberts, P., and House, L., 2001, Next-generation numerical modeling: incorporating elasticity, anisotropy and attenuation: Society of Exploration Geophysicists Annual International Meeting, Expanded Abstracts, 1218-1221.

Acknowledgements: Research supported by a 2006 Fulbright Senior Scholar award to Louie for work in New Zealand, and by GNS Science. Instruments used in the field program were provided courtesy of M. Savage of the Victoria University of Wellington, and S. Harder of the University of Texas El Paso.



Figure 1: Map of average shear velocity from the surface to 30 m depth assembled for the Wellington – Lower Hutt region of New Zealand, with the 1500 m/s velocity isosurface in shaded relief to show bedrock and basin-floor topography from Benites and Olsen (2005). Locations of 27 of 46 sites measured in 2006 for shallow shear velocity are marked with dashed circles, labeled with the measured V_{s30} in m/s. Kaiser and Louie (2006) made an additional 19 measurements in one neighborhood in the lower center of the map, with only two results shown here. The measurements allowed a revision of the shallow velocity model, with V_{s30} not exceeding 800 m/s. The basin-bounding Wellington fault runs along the northwest side of the basin.

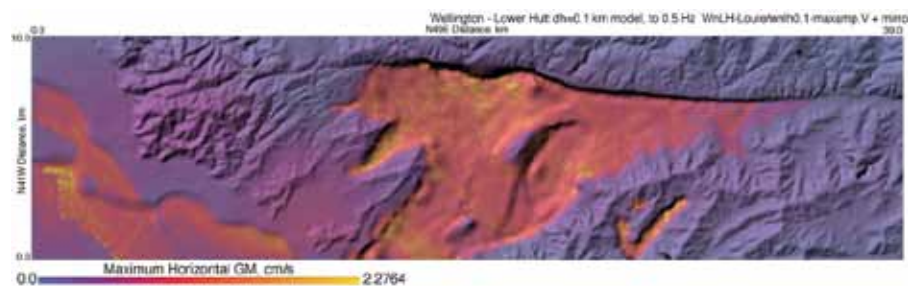


Figure 2: Map of peak ground velocity (PGV) computed for the Wellington – Lower Hutt region of New Zealand for a M3.2 event 8 km below the city, with the 1500 m/s velocity isosurface in shaded relief to show bedrock and basin-floor topography from Benites and Olsen (2005). The yellow color indicates PGV as high as 2.27 cm/s. 3D effects of complex basin geometry and soft soils are evident.

Crustal Structure beneath the High Lava Plains of Eastern Oregon and Surrounding Regions from Receiver Function Analysis

Kevin C. Eagar and Matthew J. Fouch (Arizona State University), David E. James and Richard W. Carlson (Carnegie Institution of Washington)

We analyze teleseismic P-to-S receiver functions to image crustal structure beneath the High Lava Plains (HLP) of eastern Oregon and surrounding regions. The coverage from 206 broadband seismic stations provides the first opportunity to resolve small scale variations in crustal composition, thickness, and heterogeneity. We utilize both Hk stacking and a new Gaussian-weighted common conversion point stacking technique. We find crust that is ≥ 40 km thick beneath the Cascades, Idaho Batholith, and Owyhee Plateau, and thinner (~ 31 km) crust beneath the HLP and northern Great Basin. Low Poisson's ratios of ~ 0.250 characterize the granitic Idaho Batholith, while the Owyhee Plateau possesses values of ~ 0.270 , typical of average continental crust. The Owyhee Plateau is a thick simple crustal block with distinct edges at depth. The western HLP exhibits high average values of 0.295, expected from widespread basaltic volcanism. Combined with other geological and geophysical observations, the areas of high Poisson's ratios (~ 0.320) and low velocity zones in the crust beneath north-central and southern Oregon are consistent with the presence of partial melt on either side of the HLP track, suggesting a central zone where crustal melts have drained to the surface, perhaps enabled by the Brothers Fault zone. Thicker crust and an anomalous N-S band of low Poisson's ratios (~ 0.252) skirting the Steens Mountain escarpment is consistent with residuum from a mid-crustal magma source of the massive flood basalts, supporting the view of extensive mafic under- and intraplating of the crust from Cenozoic volcanism.

References

Eagar, K.C., M.J. Fouch, D.E. James, R.W. Carlson, and the High Lava Plains Seismic Working Group, Crustal structure beneath the High Lava Plains of Eastern Oregon and surrounding regions from receiver function analysis, submitted to *J. Geophys. Res.*, June 2010.

Acknowledgements: This work would not have been possible without high quality seismic data provided through the hard work of the TA and the HLP Seismic Experiment teams (<http://www.dtm.ciw.edu/research/HLP>), and the services of the IRIS DMC. As always, the IRIS PASSCAL program provided world-class technical field support. A special thanks goes to Jenda Johnson, whose contributions to the project have been innumerable and immeasurable, and Steven Golden for providing field and data support. We would also like to acknowledge the work and productive discussions on the crustal evolution with the other PIs of the HLP project, including Anita Grunder, Bill Hart, Tim Grove, Randy Keller, Steve Harder, and Bob Duncan. This research was supported by National Science Foundation awards EAR-0548288 (MJF EarthScope CAREER grant), EAR-0507248 (MJF Continental Dynamics High Lava Plains grant) and EAR-0506914 (DEJ/RWC Continental Dynamics High Lava Plains grant).

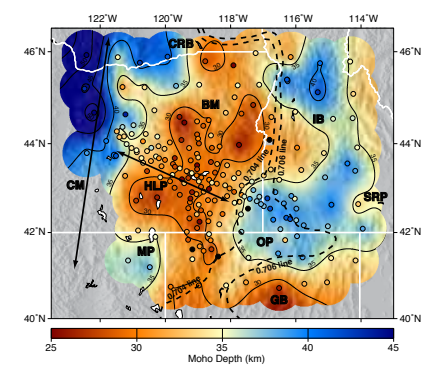


Figure 1: Map of Moho depth derived from H-k stacking analysis. Single station results (colored circles) are smoothed over a 10×10 km grid using splines under tension with a tension factor of 0.3 using the Generic Mapping Tools [Smith and Wessel, 1990]. Red colors denote shallower Moho; blue colors denote deeper Moho; gray regions represent areas of limited sampling in this study. Black solid lines denote 5 km contours. $^{87}\text{Sr}/^{86}\text{Sr}$ isopleths of 0.704 and 0.706 (“704” and “706” lines) denoted by black dashed lines. Geologic provinces include Cascade volcanic arc (CM), Blue Mountains (BM), High Lava Plains (HLP), Columbia River basin (CRB), Snake River Plain (SRP), Idaho batholith (IB), Owyhee Plateau (OP), Modoc Plateau (MP), and Great Basin (GB).

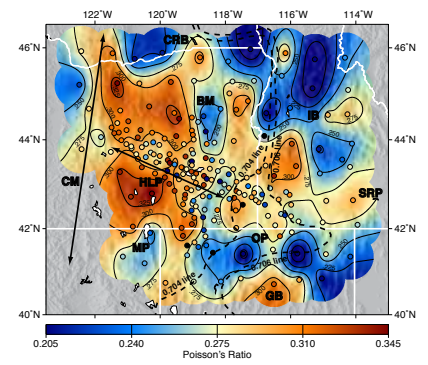


Figure 3: Map of Poisson's ratios derived from H-k stacking analysis. Smoothing parameters and geological/geochemical features are the same as in figure 1. Black solid lines denote 0.025 contours.

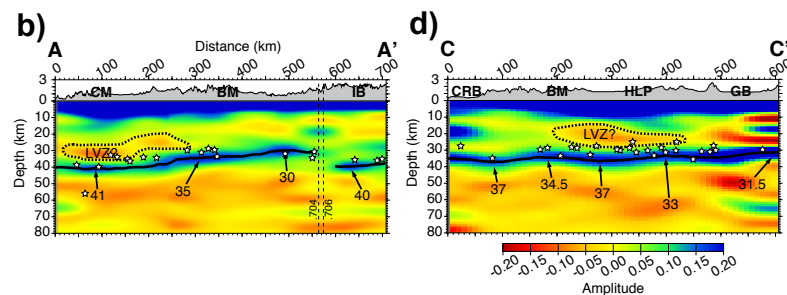
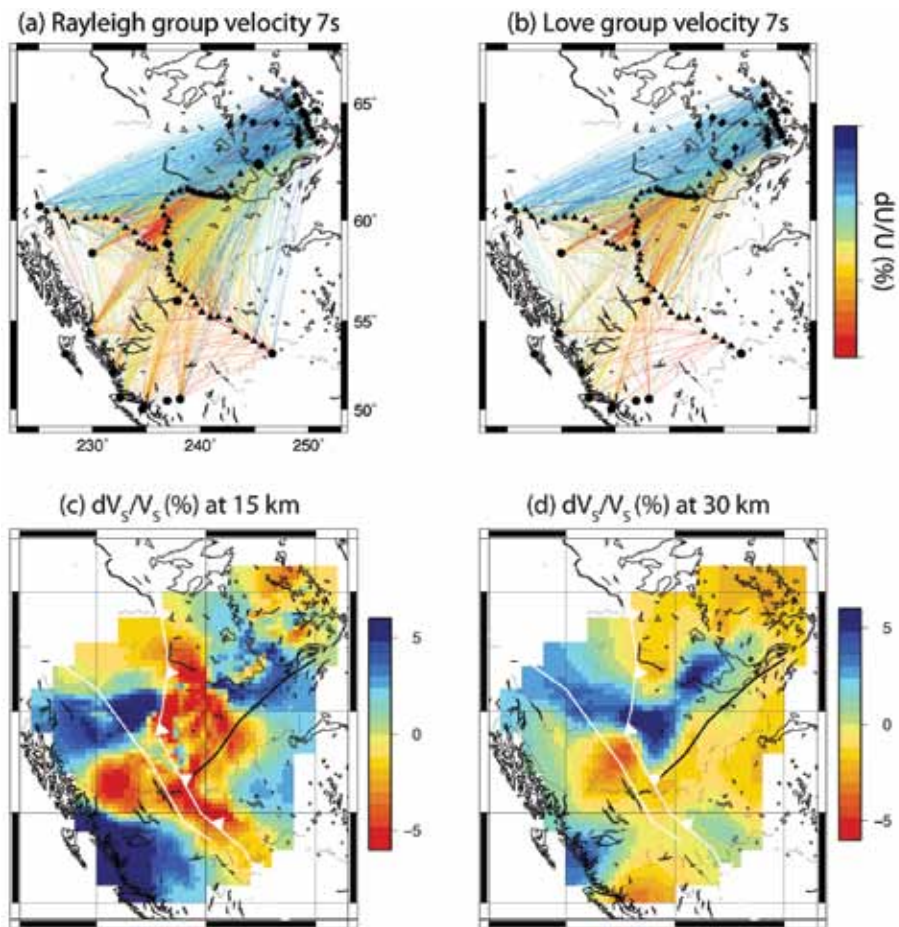


Figure 2: Cross-sections of Moho depths and crustal features. Geologic and geochemical provinces labeled as in the maps. Colored background is amplitudes from GCCP stacking. Solid line with depth labels is Moho valued picked from maximum amplitudes in GCCP stacks. Dotted black lines labeled LVZ are areas of strong negative amplitudes in the crust. White stars represent Hk Moho depths from the nearest stations along each profile. Profile A-A' is oriented east-west; profile C-C' is oriented north-south.

Imaging Radially Anisotropic Crustal Velocity Structure in NW Canada

Colleen A. Dalton (Boston University), James B. Gaherty (LDEO, Columbia University), Anna M. Courtier (James Madison University)

The tectonic evolution of Northwestern Canada spans several billion years of Earth history. As such, it presents an ideal environment for studying the processes of continental accretion and growth. We use ambient-noise cross-correlation to image anisotropic crustal seismic-velocity structure in NW Canada. Our focus area surrounds the CANOE (CANadian Northwest Experiment) array, a 16-month IRIS PASSCAL deployment of 59 broadband seismic stations. We also include 42 broadband stations from the Canadian National Seismograph Network and the POLARIS network. We estimate the Green's function for each pair of stations by cross-correlating day-long time series of ambient noise in the time period July 2004 - June 2005. We observe fundamental-mode Rayleigh waves on cross-correlated vertical-component records and Love waves on the transverse components. We measure group velocities for the surface waves in the period range 5-30 s. Laterally, group velocities vary by as much as $\pm 15\%$ at the shortest periods and $\pm 6\%$ at longer periods, with the fastest velocities found within the Slave province and very slow velocities associated with thick sedimentary layers at short periods.



(a,b) Measurements of Rayleigh and Love wave group velocity, plotted as color-coded line segments along the great-circle path connecting each station pair. Color scale ranges from 2.75-3.25 km/s and 3.0-3.6 km/s for the Rayleigh and Love waves, respectively. (c,d) Isotropic velocity perturbation in the 3-D seismic model of the study area, shown here at 15- and 30-km depth. The white and black lines indicate the Tintina fault and Great Slave Lake Shear Zone, respectively. The white barbed line shows the eastern limit of Cordilleran deformation.

We investigate 3-D shear-velocity structure using two approaches. We use a Monte Carlo approach to test whether the data are consistent with isotropic velocity and find that the Love wave data require faster velocities in the middle--lower crust than the Rayleigh waves do; i.e., $V_{SH} > V_{SV}$. We also invert the group-velocity values (> 2500 interstation paths) for 3-D radially anisotropic shear-wave velocity within the crust. Since the sensitivity kernels depend strongly on the assumed elastic structure, we use local kernels to account for the effects of laterally variable sedimentary structure. The resulting model correlates with several known geologic structures, including sedimentary basins at shallow depths and possibly the Cordillera-craton transition in the lower crust. The crustal model will also be useful for future studies of the upper mantle in this area.

Controlled-Source Seismic Investigation of the Generation and Collapse of a Batholith Complex, Coast Mountains, Western Canada

K. Wang (Virginia Tech), J. A. Hole (Virginia Tech), A. L. Stephenson (University of Victoria), G. D. Spence (University of Victoria), K. C. Miller (Texas A&M University), S. H. Harder (University of Texas, El Paso), R. M. Clowes (University of British Columbia)

In 2009, the BATHOLITHS project acquired a 400-km long refraction and wide-angle reflection seismic survey across the Coast Mountains of British Columbia, Canada, a Jurassic to Eocene continental arc batholith complex.

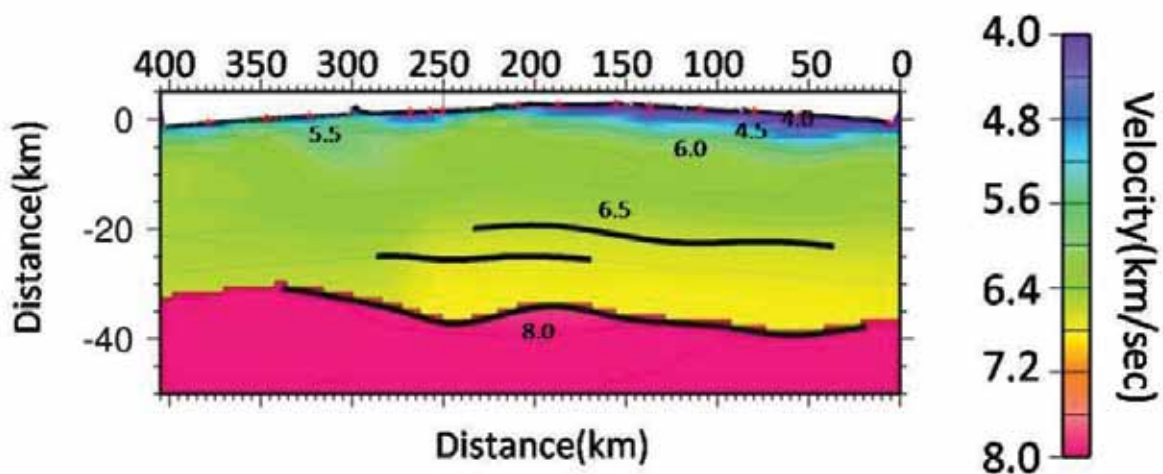
Granitic batholiths created by magmatic differentiation in arcs above subduction zones make continental crust more felsic than the original materials derived from the mantle. However, differentiation from a mafic protolith results in a large volume of ultramafic residual that is petrologically part of the crust, not changing the bulk composition. This residue may reside hidden beneath the geophysical Moho, or it may have delaminated to sink into the mantle due to its relative density. Delamination may occur during subduction or during the collapse of the arc after subduction stops, and may coincide with a commonly observed late pulse of magmatism. As part of the BATHOLITHS multi-disciplinary investigation of these processes, traveltimes from the seismic survey are being used to build a 2-D P-wave velocity model of the crust.

East of the batholith complex, surface Mesozoic sedimentary and volcanic rocks are indicated by velocities of 4-5 km/s to 2-5 km depth. Beneath this basin, the Stikine terrane, an accreted late Paleozoic to early Mesozoic island arc, has felsic seismic velocities of 5.8-6.2 km/s to at least 15 km depth. A seismic reflector is observed at ~20 km depth beneath Stikinia but does not extend into the arc complex. Based on wide-angle reflections, the lower crust has a velocity of ~6.8 km/s under Stikinia, indicating mafic rocks. The Moho is at 35-38 km depth and the upper mantle has a fast velocity of ~8.1 km/s under Stikinia.

To the west in the continental arc complex, velocities of 5.6-6.2 km/s indicate granitic rocks in the upper crust to at least 15 km depth. A strong seismic reflector is observed at ~27 km depth only beneath the highest mountains and youngest batholiths in the eastern part of the batholith complex.

Wide-angle reflections indicate a velocity <6.6 km/s above the 27-km reflector and above the Moho in the western arc complex, indicating a felsic to intermediate composition. The Moho is at 30-33 km depth under the western Coast Mountains and dips eastward to maximum of 38-40 km beneath the highest mountains. The velocity between the 27-km reflector and the deepest Moho is >6.8 km/s, but the data are currently being analyzed to better constrain this number and search for magmatic residual. The upper mantle has a slow velocity of ~7.9 km/s under the arc complex.

Acknowledgements: The BATHOLITHS controlled-source seismic project is funded by an NSF grant from the Continental Dynamics Program and by a Canadian NSERC grant.



Preliminary seismic velocity model from the BATHOLITHS controlled-source seismic survey. Lower crust and Moho structure is still being modeled, and may change from this figure. The Stikine terrane to the east of the arc extends from model km 0 to 210. The Jurassic-Cretaceous arc lies west of the Coast Shear Zone at about model km 320. The youngest arc (Cretaceous-Eocene) and highest mountains are from model km 210 to 320. The curved surface of the model represents the spherical Earth.

SIMA/PICASSO: Seismic Investigations of the Moroccan Atlas/ program to Investigate Convective Alboran Sea System Overturn

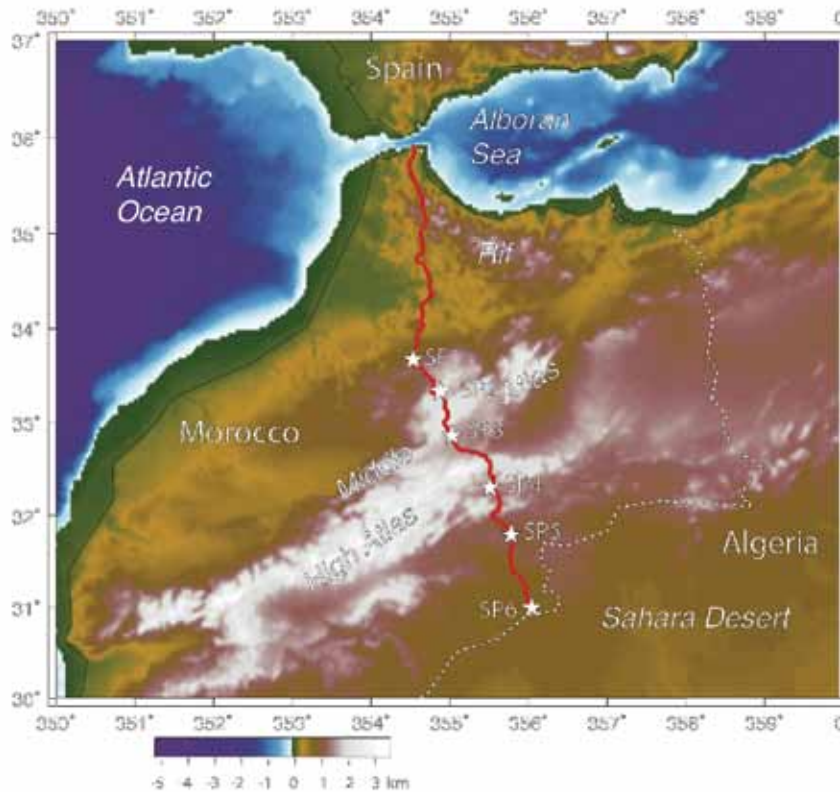
R. Carbonell (CSIC Earth Science Institute), **J. Gallart** (CSIC Earth Science Institute), **M. Harnafi** (Scientific Institute of Rabat, Rabat, Morocco), **A. Levander** (Rice University, Earth Science Department)

In April 2010 we conducted a ~500 km long seismic refraction survey extending from the Sahara Desert to the Mediterranean Sea across Morocco. The refraction profile crossed the recently uplifted High Atlas, the Middle Atlas, and the western edge of the Rif Mountains. The project, Seismic Investigations of the Moroccan Atlas (SIMA), is affiliated with the PICASSO program in Spain and Morocco.

SIMA utilized 930 Reftek 125 Texan seismographs from the PASSCAL Instrument Center. Nominal instrument spacing was 350m from El Hajeb (central Morocco) south to the Sahara, and 500m to the north. The instruments recorded six 1000 kg shots located from El Hajeb south. An internationally diverse field crew of 75 faculty and students from more than a dozen institutions in Africa, Europe, and North America conducted the 2 week long experiment. Preliminary examination of the data shows quite complicated wide-angle reflections from several levels of the crust.

PICASSO is a project that includes land and sea magnetotelluric measurements, active and passive seismic experiments, geochemical sampling, structural geology, and geodynamic investigations of the western Mediterranean, and particularly of the Betics, the Gibraltar Arc, the Alboran Sea, the Rif, and the Atlas Mountains. PICASSO institutions include Rice, USC, Oregon, and WHOI in the USA, CSIC Earth Science Institute "Jaume Almera", Barcelona, the University of Barcelona, and the University of Salamanca in Spain, the Dublin Institute for Advanced Studies in Ireland, GEOMAR and the University of Muenster in Germany, and the Scientific Institute of Rabat, in Morocco.

Acknowledgements: SIMA was funded by a grant from the Spanish Science Foundation (FECYT), and was supported as part of PICASSO by grant EAR 0808939 from the NSF Continental Dynamics Program. We thank the Scientific Institute of Rabat, Rabat, Morocco, for generous assistance in the field, and Lloyd Carothers, Mike Fort, and Lisa Foley from the PASSCAL Instrument Center for outstanding field support.



Map showing SIMA seismic refraction profile (stations are plotted in red), and shotpoints (black stars). SP1 is near El Hajeb, Morocco.

Northward Thinning of Tibetan Crust Revealed by Virtual Seismic Profiles

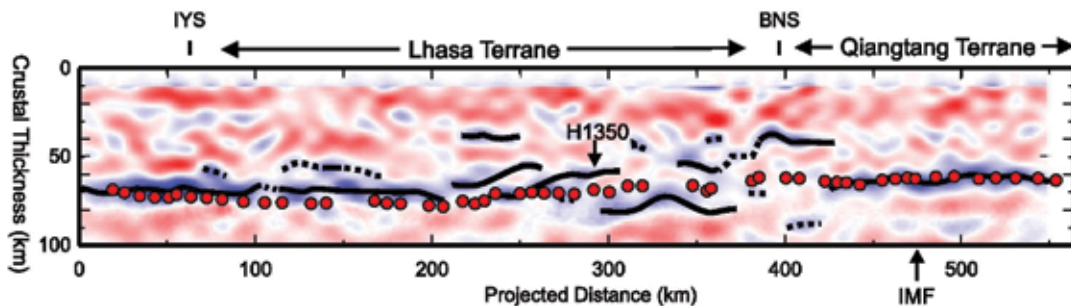
Tai-Lin Tseng (*University of Illinois, Urbana-Champaign*), Wang-Ping Chen (*University of Illinois, Urbana-Champaign*), Robert L. Nowack (*Purdue University, W. Lafayette, IN*)

A new approach of constructing deep-penetrating seismic profiles reveals significant, regional variations in crustal thickness under near-constant elevation of Tibet. Over distances of hundreds of kilometers, the crust is as thick as 75 km in southern Tibet but shoals to just over 60 km under the Qiangtang terrane in central Tibet where the deviation from Airy isostasy is equivalent to a thickness of over 10 km in missing crust. Northward thinning of crust occurs gradually over a distance of about 200 km where mechanical deformation, instead of pervasive magmatism, also seems to have disrupted the crust-mantle interface.

References

Tseng, T.-L., W.-P. Chen and R. L. Nowack, Northward thinning of Tibetan crust revealed by virtual seismic profiles, *Geophys. Res. Lett.*, 36, L24304 (with on-line supplements), doi:10.1029/2009GL040457, 2009.

Acknowledgements: The study was supported by U.S. National Science Foundation grants EAR99-09362 (Hi-CLIMB), EAR06-35419 and U.S. Air Force contract FA8718-08-C-002.



A comparison between crustal thickness estimated from wide-angle P-wave reflections (red dots) and an image of the Tibetan lithosphere obtained by Gaussian beam migration of direct P- to S-wave conversions [Nowack et al., 2010]. The convention is that a scatterer representing an increase in impedance with depth results in a blue pixel centered on the position of the scatterer. Black curves (dashed when uncertain), highlighting particularly strong impedance contrasts, show interpretations of the Moho transition zone in Nowack et al. [2009]. Notice near-constant crustal thickness over distances of hundreds of kilometers when the Moho is a simple interface near both ends of the profile. In the intervening zone of disrupted Moho, average crustal thickness decreases gradually northward by more than 10 km, from as much as 75 km to just over 60 km. Notice that the IMF is offset from the onset of shoaled Moho near the BNS. "H1350" marks the location of station whose observed waveform is discussed in detail by Tseng et al. [2009].

Quantification of Landscape Evolution Processes with Seismic Refraction Imaging, Boulder Creek Watershed, Colorado

Kevin M. Befus (*University of Colorado at Boulder*), Anne F. Sheehan (*University of Colorado at Boulder*)

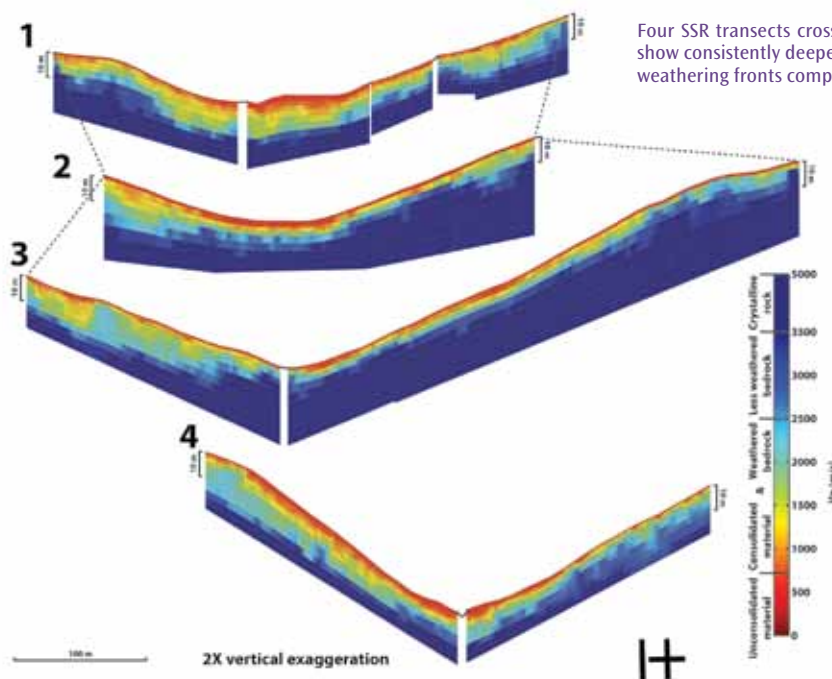
We use minimally invasive shallow geophysical techniques to image the structure of the critical zone from surface to bedrock (0-25 m) throughout two small drainages within the Boulder Creek Critical Zone Observatory (BcCZO). Shallow seismic refraction (SSR) reveals the physical characteristics of the shallow subsurface. Results of the SSR surveys provide a pseudo-3D network of critical zone compressional wave velocity (V_p) structure within each catchment.

The evolution of each catchment within the BcCZO contain signals of both erosion and weathering dependent upon the large-scale geomorphic processes down to the microbial weathering of mineral grains. The geophysical approach describes the arena for the small-scale processes while also providing a quantitative description of the critical zone structure at an instant in time. This study encompasses two catchments, Betasso and Gordon Gulch, with connected recent and continuing geomorphic processes: fluvial rejuvenation and long-term quiescent erosion, respectively.

Geophysical results show crystalline bedrock V_p was greater than 3500 m/s, unconsolidated material V_p was generally less than 700 m/s and various gradients of weathered bedrock and consolidated material ranged from 700-3500 m/s if present. Fresh bedrock values in Betasso were imaged 12.1 ± 2.8 m below the ground surface. Moderately weathered bedrock ($V_p > 2000$ m/s) was imaged at 6.0 ± 2.4 m depth. Weathered rock and consolidated materials were imaged at 3.4 ± 1.8 m depth. Unconsolidated materials were generally thinner than the sensitivity of our line setup at 0.9 ± 0.8 m thick. In Gordon Gulch fresh bedrock values were imaged 11.7 ± 3.1 m below the ground surface, moderately weathered bedrock at 5.8 ± 2.7 m depth, and weathered rock and consolidated materials at 3.2 ± 1.9 m depth. Again, unconsolidated materials were generally thinner than the sensitivity of our line setup at 0.9 ± 0.7 m thick.

Significant topography and irregular bedrock surfaces contribute additional complexity to the critical zone architecture in each catchment. Aspect driven differences in the subsurface within each catchment overprints the broader geomorphic signals. SSR subsurface structure models will guide future investigations of critical zone processes from landscape to hydrologic modeling and assist in expanding point measurements of physical, chemical, and biological processes to the catchment scale.

Acknowledgements: I appreciate working as a research assistant as part of the Boulder Creek Critical Zone Observatory (BcCZO) funded by NSF grant NSF-EAR 0724960. I acknowledge the Mentorship Program of the University of Colorado's Department of Geological Sciences and the BcCZO in funding my field assistants. Also, I thank Austin Andrus for taking time out of working on his own related IRIS project to assist me with my fieldwork. I appreciate IRIS Pascal for loaning Geometrics Geode seismic equipment and field computers with important analysis software.



An Integrated Analysis of an Ancient Plate Boundary in the Rocky Mountains

Eva-Maria Rumpfhuber (*University of Oklahoma*), Randy Keller (*University of Oklahoma*)

Integration of multiple data sets to obtain better resolved, multiple parameter earth models has recently received new emphasis. We conducted an integrated analysis of the controlled-source seismic (CSS) and passive source seismic data from the CD-ROM (Continental Dynamics of the Rocky Mountains) experiment along with gravity and seismic reflection data. A specific goal of this study was establish a stronger tie between the CD-ROM and Deep Probe experiments that together form a profile that extends from northern New Mexico to Alberta, Canada. A major advantage of the CD-ROM seismic experiment dataset was the coincidence of the seismic profiles (Fig. 1), which facilitated a joint interpretation of our new results and the previous CD-ROM results. As the first step in this process, we created a new P-wave velocity and interface model from the CSS data based on an advanced picking strategy that produced a new and extended set of travel-time picks relative to those employed in previous studies. In addition, we were able to identify a substantial set of S-wave arrivals and establish an independent S-wave model. Thus, we were able to compare and jointly interpret crustal thicknesses the various techniques produced as well as v_p/v_s ratios from receiver functions and the CSS dataset. Furthermore, the comparisons provided insights about the strengths and uncertainties of each technique. Thanks to the integration of the controlled-source and receiver function results, we were able to construct a well-constrained structural model and tectonic interpretation that shows the structural framework of the transition from the Wyoming craton to the north across the suture Cheyenne belt suture zone into the Proterozoic terranes to the south (Fig. 2). The interpretation that crustal-scale crocodile structures are present provides an explanation for the south dip of the Cheyenne belt suture in the upper crust and the north-dipping slab in the mantle (Fig. 2). The very distinct crustal structures north and south of the suture zone are clearly shown in our model and document that the blocks that collided ~1.8 Ga to form the Cheyenne belt suture zone have retained their basic crustal and uppermost mantle structure since that time.

Acknowledgements: This work was supported by the National Science Foundation as part of the GEON project (EAR-0225670)

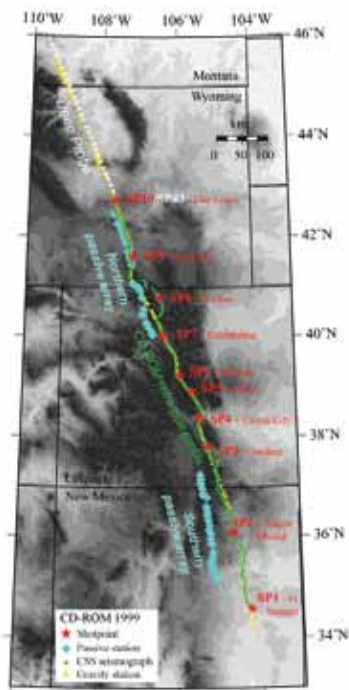


Figure 1: Index map of the CD-ROM seismic experiments. The controlled source seismic stations (green), their corresponding shotpoints (red stars), and the northern and southern passive arrays (light blue diamonds) are shown. Yellow dots indicate the locations of gravity stations. The Deep Probe experiment profile that also used the Day Loma shotpoint is shown as a white dashed line.

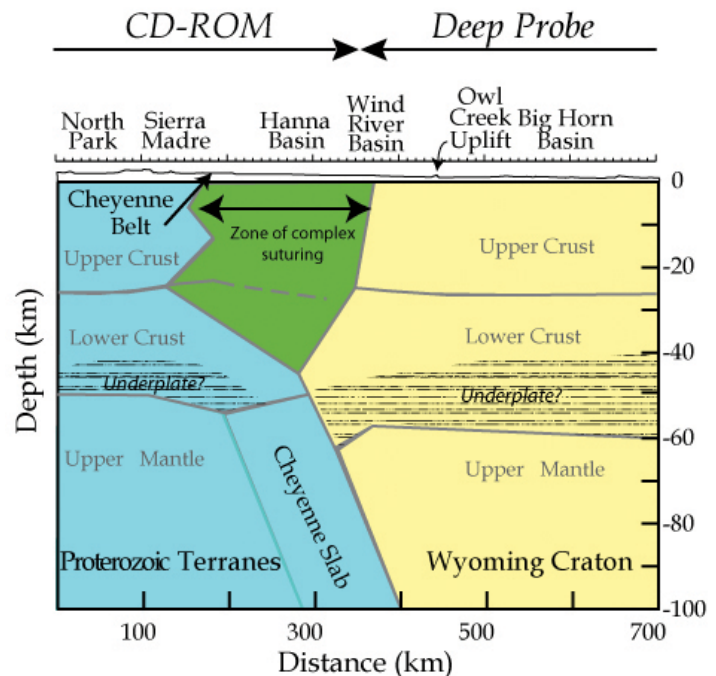


Figure 2: Tectonic synthesis based on the integration of the seismic data from the CD-ROM and Deep Probe experiments. The yellow color indicates the Wyoming Craton in the north, and the blue color represents the Proterozoic terranes to the south. An area of complex suturing (Crocodile structure) is indicated in green. The horizontal lined pattern in the lower crust indicates interpreted zones of underplated material based on xenolith data.

Full-Wave Ambient Noise Tomography of Northern Cascadia

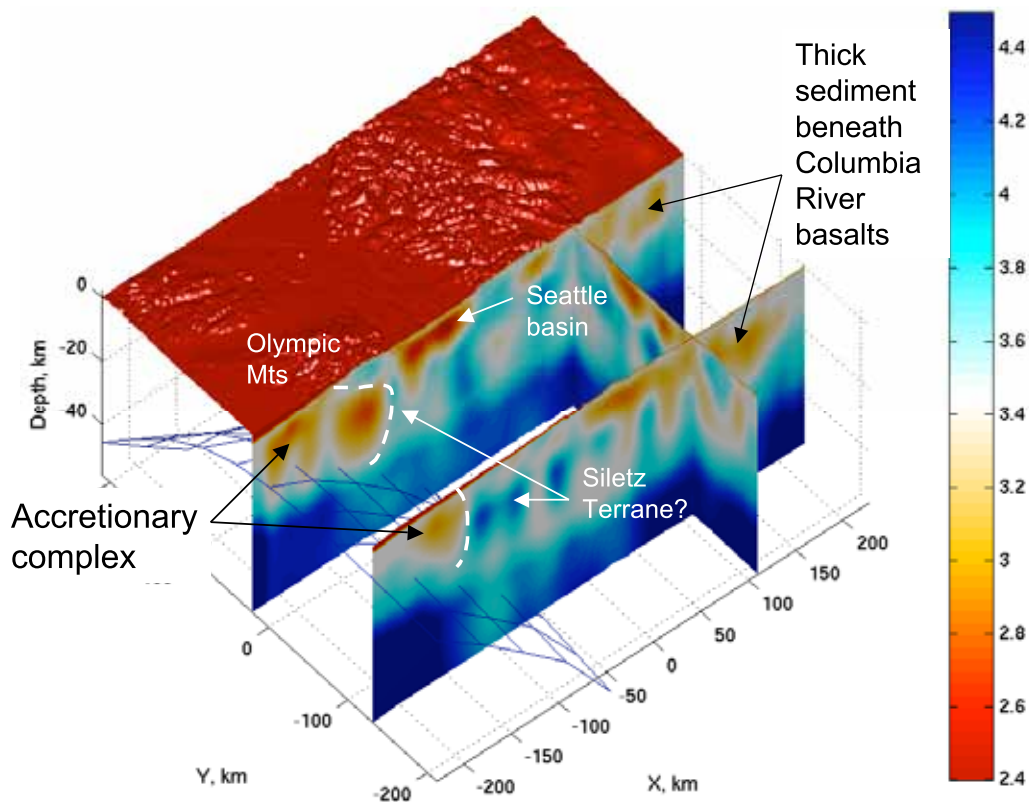
Yang Shen (University of Rhode Island), Wei Zhang (University of Rhode Island)

We use empirical Green's functions derived ambient noise to iteratively improve a 3D velocity model of the crust and uppermost mantle beneath northern Cascadia. The data set includes up to 5 years (2005-2009) continuous records from 69 broadband seismic stations. Wave propagation is simulated using a finite-difference method with boundary conforming grids that account for the effects of topography and 3D heterogeneity. The initial reference model is CRUST 2.0. Travel time anomalies are measured by cross-correlating empirical and synthetic Green functions. Finite-frequency sensitivity kernels are computed using the scattering integral method. In the frequency and time window of interest, the empirical Green's function derived from cross-correlation of vertical-to-vertical component is dominated by Rayleigh waves, which are sensitive to not only shear but also compressional wave speeds. So the inverse problem is structured as a joint solution for V_p and V_s . The solution converges after 4 model iterations, with a total 96% variance reduction. Resolution tests show a V_p resolution in the shallow crust. The V_p structure is validated by a comparison with active-source experiments and well logs. A comparison of the observed and predicted earthquake waveforms shows a much-improved waveform fit, indicating that the new model could be used to refine seismic hazard assessment. The new model also reveals features that relate to geological observations, such as the sediment basins, the accretionary complex and the Siletz terrane.

References

Shen, Y., and W. Zhang (2010), Full-wave ambient noise tomography in Northern Cascadia, *Seismol. Res. Lett.*, 81 (2), SSA 2010 Abstract.

Acknowledgements: This research was supported by the National Science Foundation under grant 0727919 and the Air Force Research Laboratory under contract FA9453-10-C-0217. The IRIS DMC provided seismic waveforms.



The 3D shear velocity model of northern Cascadia from full-wave ambient noise tomography. The mesh represents the upper surface of the subducted oceanic crust. Color indicates the wave speed in km/s. Several geological features are clearly imaged, such as the Seattle Basin, the accretionary complex, the Siletz Terrane and the sediment beneath Columbia River basalts.

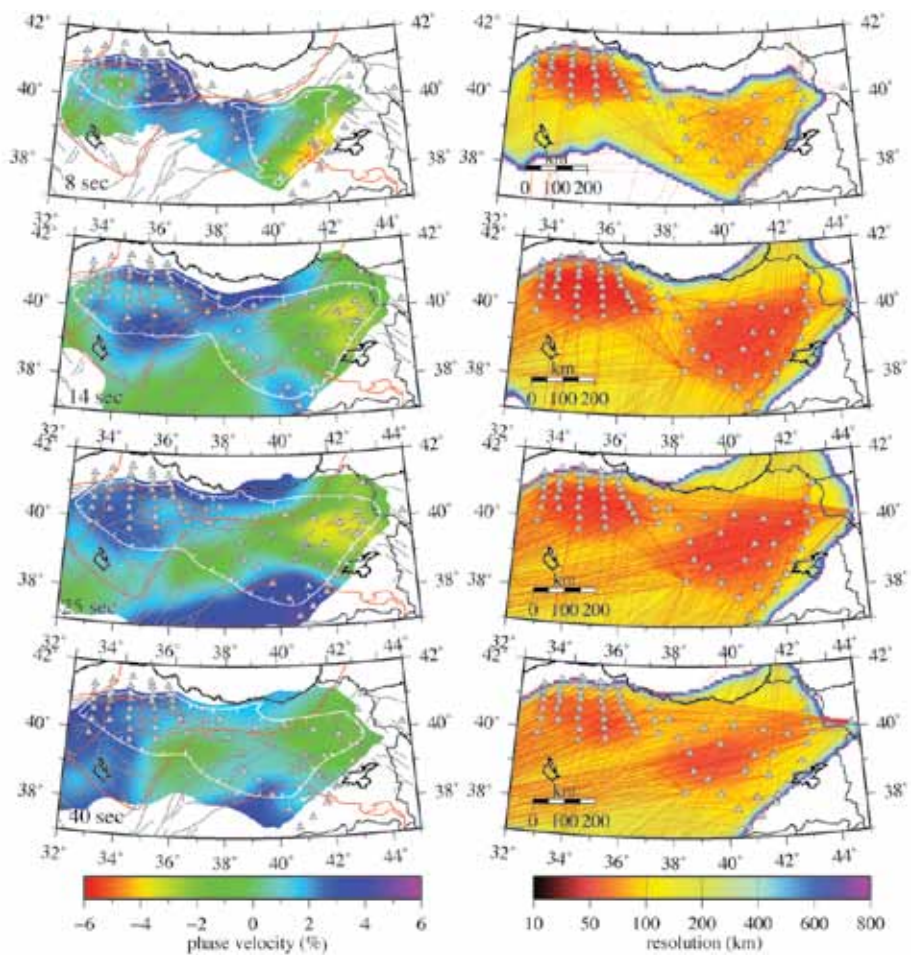
Crustal Velocity Structure of Turkey from Ambient Noise Tomography

Linda M. Warren (*Saint Louis University*), Susan L. Beck (*University of Arizona*), George Zandt (*University of Arizona*), C. Berk Biryol (*University of Arizona*), A. Arda Ozacar (*Middle Eastern Technical University*), Yingjie Yang (*University of Colorado*)

In eastern Turkey, the ongoing convergence of the Arabian and African plates with Eurasia has resulted in the westward extrusion of the Anatolian plate. To better understand the current state and the tectonic history of this region, we image crust and uppermost mantle structure with ambient noise tomography. Our study area extends from longitudes of 32-44 degrees E. We use continuous data from two PASSCAL deployments, our 2006-2008 North Anatolian Fault Passive Seismic Experiment and the 1999-2001 Eastern Turkey Seismic Experiment, as well as from additional seismometers in the region. We compute daily cross-correlations of noise records between all station pairs and stack them over the entire time period for which they are available, as well as in seasonal subsets, to obtain interstation empirical Green's functions. After selecting interstation cross-correlations with high signal-to-noise ratios and measuring interstation phase velocities, we compute phase velocity maps at periods ranging from 8-40 s. At all periods, the phase velocity maps are similar for winter and summer subsets of the data, indicating that seasonal variations in noise sources do not bias our results. Across the study area, we invert the phase velocity estimates for shear velocity as a function of depth. The shear velocity model, which extends to 50 km depth, highlights tectonic features apparent at the surface: the Eastern Anatolian Volcanic Province is a prominent low-velocity anomaly whereas the Kirsehir Block has relatively fast velocities. In addition, in the southeastern part of our study area, we image a high velocity region below 20 km depth which may be the northern tip of the underthrusting Arabian plate. There are velocity jumps across the Central and East Anatolian Fault Zones. The North Anatolian Fault Zone appears as a fast anomaly in the upper crust.

Acknowledgements: This work was funded by the National Science Foundation through grant EAR-0309838 and Independent Research and Development time.

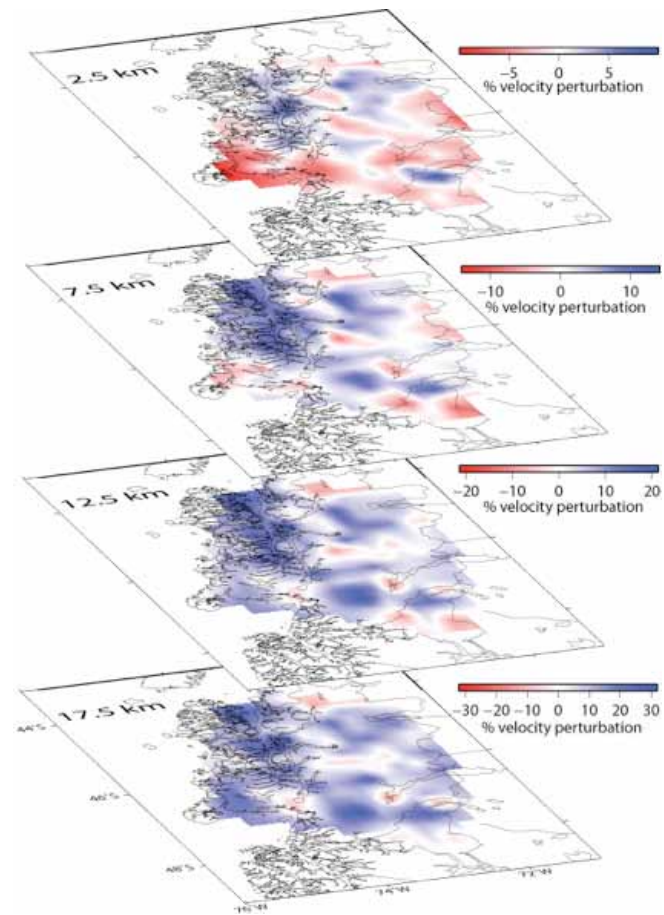
Phase velocity (left column) and horizontal resolution maps (right column) for periods of 8, 14, 25, and 40 s. Phase velocity maps, with period labeled in the lower left, show percent variations relative to the mean phase velocity. Phase velocities are plotted for regions with horizontal resolution ≤ 150 km, with white contour lines showing regions with resolution ≤ 100 km. Stations (gray triangles), faults (gray lines), and paleo-sutures (red lines) are also shown. The resolution maps in the right column show path coverage (red lines) and horizontal resolution.



Seismic Noise Tomography in the Chile Ridge Subduction Region

A. Gallego (University of Florida), R. M. Russo (University of Florida), D. Comte (Universidad de Chile), V. I. Mocanu (University of Bucharest), R. E. Murdie (Goldfields Australia), J. C. Vandecar (DTM -Carnegie Institution of Washington)

We used cross-correlation of ambient seismic noise recorded in the Chile Triple Junction (CTJ) region to estimate inter-station surface wave time-domain Green's functions, and then inverted travel times to obtain crustal surface wave velocity models. Inter-station distances within the Chile Ridge Subduction Project temporary seismic network ranged from 40 to ~100 km. We selected 365 days, and cross-correlated and stacked 24 hours of vertical component data at 38 stations pairs, resulting in nominally 703 travel-times along assumed-straight inter-station paths. Velocities in two-dimensional cells of 30 x 30 km were calculated using a linear least-squares inversion of the Rayleigh wave travel times. Furthermore we performed a Rayleigh wave dispersion analysis to estimate the sensitivity of different period waves at depth and to calculate a 3D model of the Patagonian crust. The process was applied to cross correlation pairs determined in two period bands, 5-10 sec, corresponding to shallow crustal velocities down to approximately 10 km depth, and 10-20 sec, for velocities down to around 20 km. Our results show that cell velocities correlate well with known geologic features: We find high crustal velocities where the Patagonian Batholith outcrops or is likely present at depth, and low velocities correlate with the active volcanic arc of the Southern Volcanic Zone and the subducted Chile ridge, where thermal activity is present. High velocities in the mountainous portions of the southeastern study area appear to correlate with outcropping older metamorphic units. Low velocity in the east correlate with sequences of volcanoclastic deposits.



3-D inversion derived from dispersion analysis; the color bands correspond to the percentage variation with respect to the calculated 1-D model

References

Gallego, A., R. M. Russo, D. Comte, V. Mocanu, R. Murdie, and J. VanDecar, Seismic noise tomography in the Chile Ridge Subduction region, accepted for publication in *Geophysical Journal International*, 03 June 2010.

Acknowledgements: This work was supported by U.S. National Science Foundation grant EAR-0126244 and CONICYT-CHILE grant 1050367.

Ambient Noise Tomography of the Pampean Flat Slab Region

Ryan Porter (*University of Arizona*), George Zandt (*University of Arizona*), Susan Beck (*University of Arizona*), Linda Warren (*Earthscope Program, Division of Earth Sciences, NSF*), Hersh Gilbert (*Purdue University*), Patricia Alvarado (*Universidad Nacional de San Juan*), Megan Anderson (*Colorado College*)

Ambient noise tomography is a recently developed seismic analysis technique that uses background noise to approximate the seismic velocities with a region. We apply this technique to a study of the Pampean flat slab region (Fig. 1) to better understand crustal features related to the convergence of the Nazca and South American Plates. Flat slab subduction has led to a shut-off of arc magmatism and a migration of deformation inboard from the plate margin. The region's crust is composed of several terranes accreted on the Rio de la Plata craton with zones of thin-skinned deformation in the Precordillera and thick-skinned deformation in the Sierras Pampeanas. The purpose of this work is to use ambient noise to better understand the role these features play in the region's tectonic evolution. Ambient noise tomography is based on the principal that the cross-correlation of seismic noise recorded at two seismic stations can approximate the Green's function between the stations. This noise is generally associated with ocean waves colliding with the coast. We use the ambient noise to calculate Rayleigh wave dispersion curves and convert those measurements into shear wave velocities. A detailed description of the method is found in Benson et al. [2007]. Two advantages of ambient noise over traditional surface wave tomography are that it produces a higher quality signal at shorter periods and it does not require earthquakes at certain backazimuths and distances. Initial results from this work suggest that shear wave velocities in the upper crust are primarily controlled by the presence of (slow) basins and (fast) bedrock exposures and that these basins may extend as deep as ~10-12 km (Fig 2). Lower velocities are observed beneath the shutoff volcanic arc than in the Sierras Pampeanas suggesting that a) the presence of arc related rocks is retarding seismic velocities or b) that the differences in Moho depth is impacting the measured seismic velocities. We generally observe faster seismic velocities in areas of thick-skinned deformation than in thin-skinned areas. This is especially true beneath the Precodillera, which has accommodated 60–75% of the surface shortening since 10 Ma [Allmendinger, 1990], and exhibits relatively slow velocities down to 30 km, suggesting that deformation is preferentially focused in this low velocity region.

References

- Allmendinger, R., D. Figueroa, D. Snyder, J. Beer, C. Mpodozis, and B. Isacks (1990), FORELAND SHORTENING AND CRUSTAL BALANCING IN THE ANDES AT 30°S LATITUDE, *Tectonics*, 9(4), 789-809.
- Anderson, M.L., Alvarado, P., Zandt, G., Beck, S. (2007), Geometry and brittle deformation of the subducting Nazca Plate, Central Chile and Argentina. *Geophys. J. Int.*, 171, 419-434.
- Bensen, G.D., M.H. Ritzwoller, M.P. Barmin, A.L. Levshin, F. Lin, M.P. Moschetti, N.M. Shapiro, and Y. Yang (2007), Processing seismic ambient noise data to obtain reliable broad-band surface wave dispersion measurements, *Geophys. J. Int.*, 169, 1239-1260.

Acknowledgements: This work was funded by NSF award #0510966.

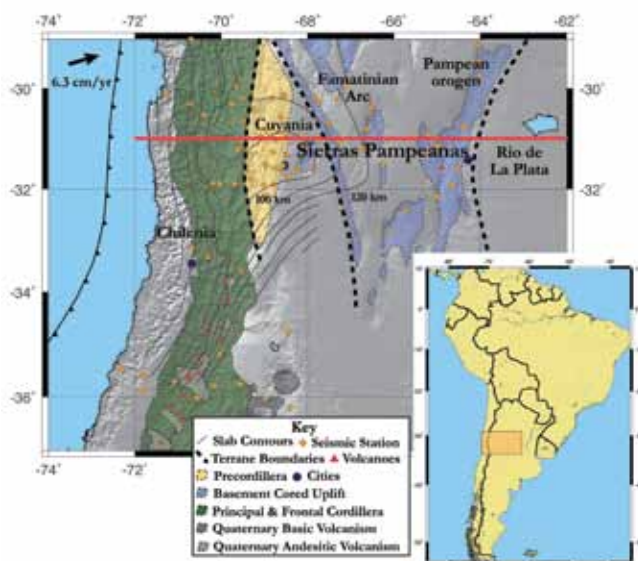


Figure 1. Location map of the study area. Red line shows location of cross section in Figure 2. Slab contours from Anderson (2007).

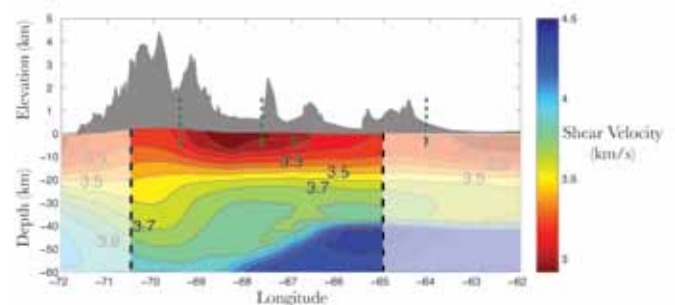


Figure 2. Cross-section of shear wave velocities at 31 degrees S. (Location shown in Figure 1). The low velocities observed above the Moho at -66 to -68 degrees are likely due to uncertainties in Moho depth. Measurements are corrected for topography and zones with less than 100 km resolution are shaded out. Green dashed lines show surface locations of terrane boundaries. Topography is exaggerated 10x.

Pacific Northwest Crust and Lithosphere Structure Imaged with Ambient Noise Tomography

Haiying Gao (*University of Oregon*), Eugene Humphreys (*University of Oregon*), Huajian Yao (*Mass. Inst. of Tech.*), Robert van der Hilst (*Mass. Inst. of Tech.*)

Rayleigh-wave ambient noise tomography from periods 6-40 seconds is used to study the Pacific Northwest crust and uppermost mantle structures with the methods of Yao et al. [2006]. We include a total of about 300 broadband stations recording from 2006-2009, including EarthScope US Transportable Array, the Wallowa flex-array, a portion of the High Lava Plains flex array, and seven permanent stations. The western U.S. model of Yang et al. [2008] is used for shear-wave velocity reference. We focus on three areas:

1) Cascades. In the Washington Cascades, where magmatic production diminishes northward to low values, the upper crust near magmatic centers usually is fast and the lower crust is slow. In Oregon, magmatic production rate is high and the crust and upper mantle are slow, whereas the old western Cascades upper crust is quite fast. These observations are consistent with the idea that magmatic intrusions make crust fast, but that high temperature can be dominant.

2) Pasco Basin. The upper crust is very slow, suggesting that this deep sedimentary basin (which is covered by Columbia River flood basalt flows) is larger than previously mapped.

3) Siletzia. The fast lower crust and upper mantle of eastern Washington and north-central Oregon is attributed to Siletzia, a fragment of ocean lithosphere that accreted ~ 50 Ma. The SE boundary of Siletzia (the Klamath-Blue Mountains gravity lineament; dashed line) is thought to represent a transform suture, and is well defined by the tomography. The NE suture is thought to be a subduction thrust system that trends NW to Vancouver Island (dotted line). We suggest that eastern Washington's low-lying (see dash-dot line), tectonically rigid and seismically faster lower crust and upper mantle is under-thrust Siletzia lithosphere.

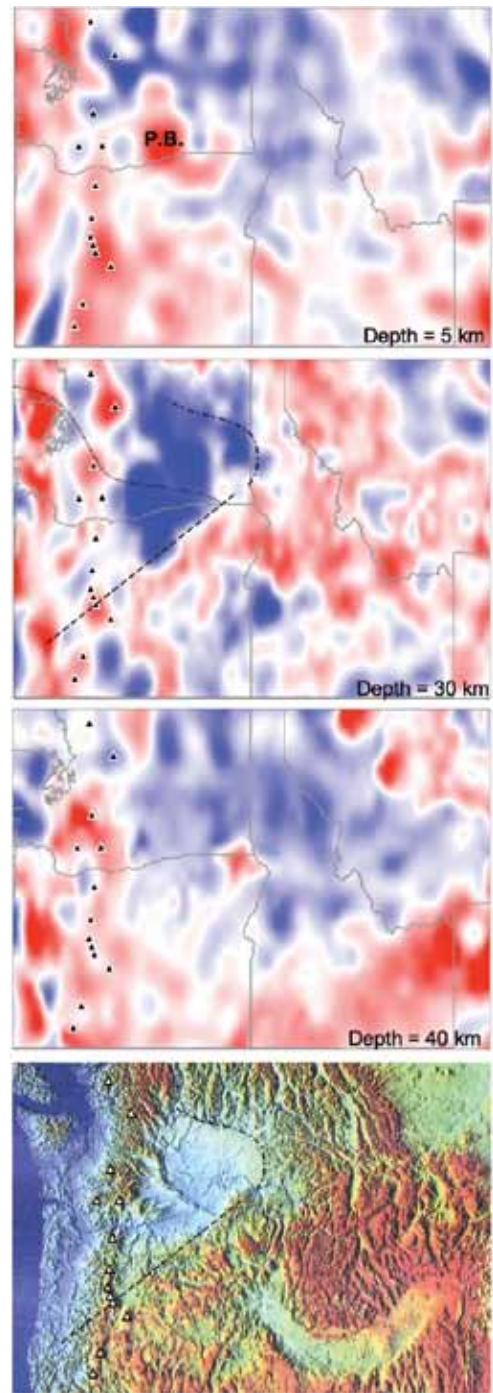
References

Yang, Y., Ritzwoller, M.H., Lin, F.-C., Moschetti, M.P., and Shapiro, N.M., Structure of the crust and uppermost mantle beneath the western United States revealed by ambient noise and earthquake tomography, *J. Geophys. Res.*, 113, doi:10.1029/2008JB005833, 2008.

Yao, H., van der Hilst, R.D., and de Hoop, M.V., Surface-Wave array tomography in SE Tibet from ambient seismic noise and two-station analysis – I. Phase velocity maps, *Geophys. J. Int.*, 166(2), 732-744, doi:10.1111/j.1365-246X.2006.03028.x., 2006.

Gao, H., E. D. Humphreys, H. Yao, and R. D. van der Hilst, Crustal and lithosphere structure of the Pacific Northwest with ambient noise tomography, in prep.

Acknowledgements: This research is supported by NSF award EAR-051000.



Tomography maps show the inverted isotropic shear-wave velocity structures (perturbations of ± 0.5 km/s relative to the average velocity; blue is fast). Triangles show the Quaternary volcanoes of the Cascade arc, and P.B. is the Pasco Basin.

Ambient Noise Monitoring of Seismic Speed

Michel Campillo (*Université Joseph Fourier and CNRS, Grenoble, France*), Nikolai Shapiro (*IPGP and CNRS, Paris, France*), Florent Brenguier (*Observatoire Volcanologique de la Réunion*), Matthieu Landes (*CEA, Bruyère-le-Chatel*)

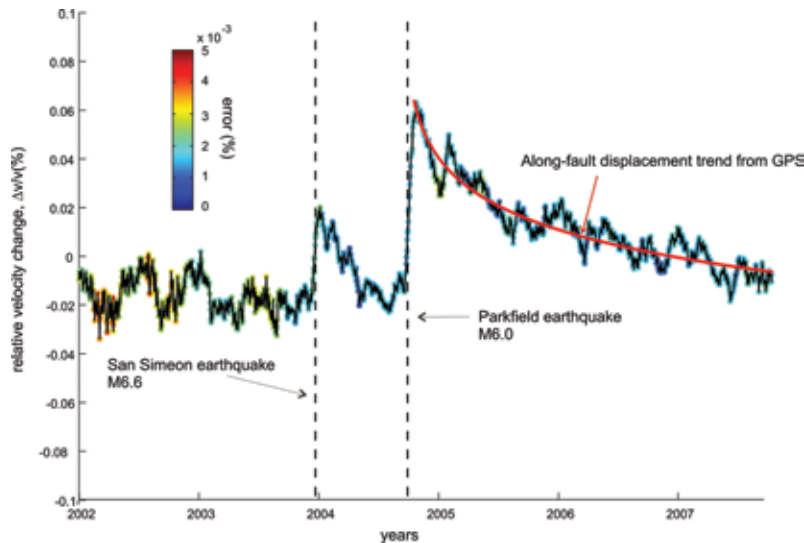
With the availability of continuous recordings from numerous seismological networks, it is now possible to use the ambient seismic noise to monitor the temporal evolution of mechanical properties of the Earth's crust. As an example, we show the detection of co-seismic and post seismic change of seismic speeds associated with the 2004 Parkfield earthquake based on correlations of seismic noise recorded by stations of the High Resolution Seismic Network [Brenguier et al., 2008]. The velocity drops at the time of the earthquake, and recovers slowly during the next years. The similarity of the time evolution of the velocity anomaly with the strain measured by GPS suggests that the velocity change can be associated to both the well-documented response of shallow layers to strong motions, and the strain at depth. Changes of velocity are small and a high precision of measurement is required. Specifically, we must separate the effect of changes at depth and the apparent changes due to the temporal migration of the sources of noise. The latter can be also studied from the analysis of long continuous seismic recordings available at international data centers such as IRIS DMC [e.g. Landes et al., 2010].

References

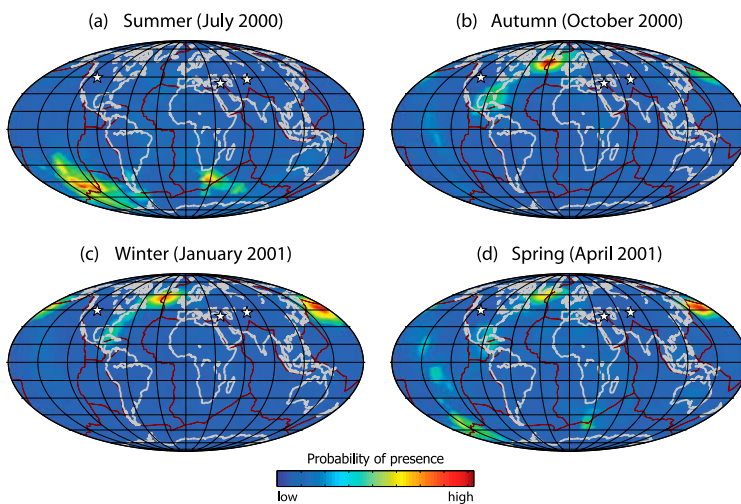
Brenguier F, M. Campillo, C. Hadziioannou, N.M. Shapiro, R.M. Nadeau, E. Larose (2008), Postseismic relaxation along the San Andreas fault in the Parkfield area investigated with continuous seismological observations *SCIENCE*, 321 (5895), 1478-1481.

Landes M, Hubans F, Shapiro NM, Paul A., and M. Campillo Origin of deep ocean microseisms by using teleseismic body waves *J. Geophysical Res.* 115: B05302, 2010

Acknowledgements: This work is supported by the European Research Council Advanced Grant WHISPER



Top: Temporal evolution of the velocity in the region of Parkfield for the period 2002-2008 (see Brenguier et al. 2008 for details). Bottom: an example of the seasonal variation of the sources of secondary microseisms obtained from teleseismic body waves (see Landes et al. 2010 for details).



Vp Structure of Mount St. Helens Imaged with Local Earthquake Tomography

Gregory Waite (*Michigan Technological University*), Seth Moran (*USGS*)

We present a new P-wave velocity model for MSH using local earthquake data recorded by the Pacific Northwest Seismograph Stations and Cascades Volcano Observatory since the 18 May 1980 eruption. These data were augmented with records from a dense array of 19 temporary stations deployed during the second half of 2005. Between June 1980 and the September 2004, 19,379 earthquakes were located by the PNSN within a 50 km by 50 km area centered on MSH. An additional 6916 events were located in this area between October 2004 and the end of 2005, which represents a small fraction of the total number of events associated with the 2004-2008 eruption. The large number of earthquakes in the catalog permits a careful selection of data for only the best-quality 7798 events. Because the distribution of earthquakes in the study area is concentrated beneath the volcano and within two nearly linear trends, we used a graded inversion scheme to compute a coarse-grid model that focused on the regional structure, followed by a fine-grid inversion to improve spatial resolution directly beneath the volcanic edifice.

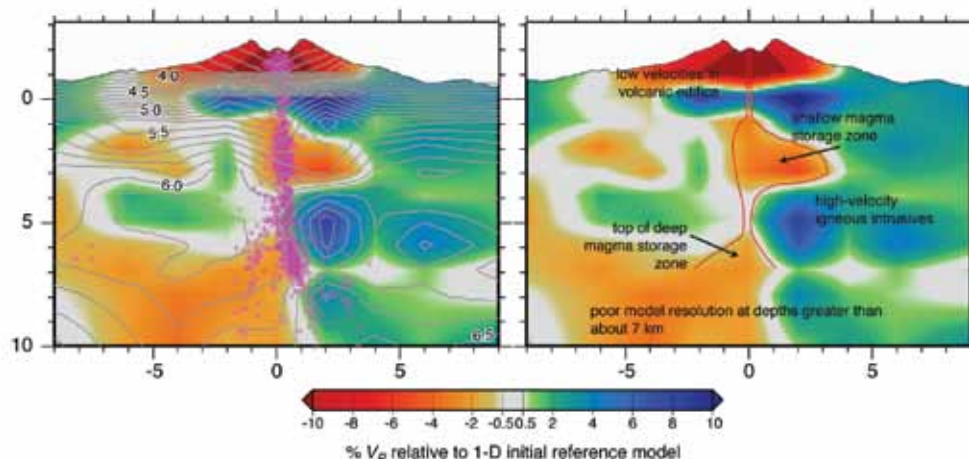
The well-resolved velocity anomalies below MSH are generally consistent with previous studies that have found two igneous intrusive bodies NE and NW of the edifice, and a structural boundary that parallels the SHZ. North of MSH, the SHZ is bounded by a low-velocity anomaly to the west and the Spirit Lake Pluton to the east. The coincidence of the velocity anomalies and the trend of earthquakes strengthens the argument that MSH sits along a significant NNW-trending structural anomaly [*e.g.*, Parsons *et al.*, 1999].

Small-scale features of the magmatic system were less well resolved, but a significant low-velocity zone from 1-3 km bsl may be due to a shallow magma-storage reservoir (Figure 1). A strong high-velocity anomaly, previously interpreted as a magma plug [Lees, 1992] was found to be east of the vertical zone of earthquakes directly beneath MSH instead of within the earthquake zone. This anomaly may be attributed to crystallized magma, but we do not interpret it as a plug within the conduit. The deeper low-velocity anomaly that we interpret as part of the magma storage system is poorly resolved due to the lack of deep earthquakes, but is consistent with earlier suggestions that the earthquake-free region is likely to be magma rich.

References

- Lees, J.M. (1992), The magma system of Mount St. Helens; non-linear high-resolution P-wave tomography, *J. Volcanol. Geotherm. Res.*, 53, 103-116.
- Parsons, T., R.E. Wells, M.A. Fisher, E. Flueh, and U.S. ten Brink (1999), Three-dimensional velocity structure of Siletzia and other accreted terranes in the Cascadia forearc of Washington, *J. Geophys. Res.*, 104(B8), 18,015-18,039.
- Waite, G. P., and S. C. Moran (2009), VP Structure of Mount St. Helens, Washington, USA, Imaged with Local Earthquake Tomography, *J. Volcanol. Geotherm. Res.*, 182(1-2), 113-122.

Acknowledgements: We thank the staff at the PNSN for their dedication to providing high-quality data and IRIS-PASSCAL Instrument Center for providing instruments and support for the temporary network. Data collected will be available through the IRIS Data Management Center. The facilities of the IRIS Consortium are supported by the National Science Foundation under Cooperative Agreement EAR-0552316, the NSF Office of Polar Programs and the DOE National Nuclear Security Administration.



A west-east cross section through a single fine-grid model highlights the low velocity anomaly directly beneath the volcano. There is no vertical exaggeration.

Mushy Magma beneath Yellowstone

Risheng Chu (California Institute of Technology), Don Helmberger (California Institute of Technology), Daoyuan Sun (California Institute of Technology), Jennifer M. Jackson (California Institute of Technology), Lupei Zhu (Saint Louis University)

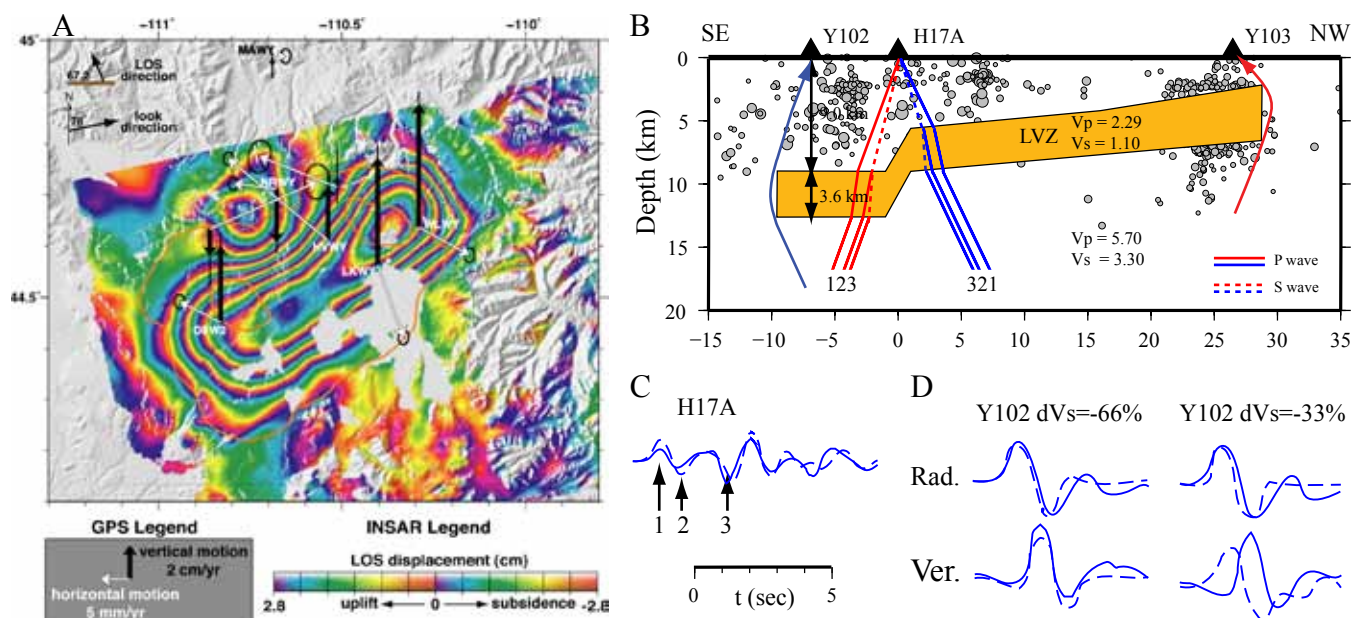
Recent GPS and InSAR studies show that the Yellowstone caldera is uplifting at a rate of 7 cm/year, which is apparently related to a magma recharge (Fig. A) [Chang *et al.*, 2007]. Seismic tomographic studies, however, claim a high degree of crystallization of the underlying magma body based on velocities inferred from regional seismic data. In this research, we analyzed receiver functions recorded by EarthScope station H17A from 100 teleseismic earthquakes in 2008. Two P-to-SV converted phases that correspond to the top and bottom of a low velocity layer (LVL) are identified (Fig. B-C). After modeling these phases, we found the LVL at about 5 km depth beneath the caldera. P- and S-wave velocities are 2.3 km/sec and 1.1 km/sec, respectively. This shallow LVL beneath the Yellowstone Caldera is severe enough to cause difficulties with seismic tool applications. In particular, seismologists expect teleseismic P waves to arrive with motions up and away or down and back. Many of the observations recorded by the YISA PASSCAL array violate this assumption. Stations near the trailing edge have reversal radial-component motions, while stations near the leading edge do not (Fig. D). Synthetic wave propagation show that it is the edge of the LVL that are sharp enough for P wave to wrap around the ends to reach the receivers before the direct arrivals. If the velocity drop is not severe enough, radial and vertical components have the same polarities (Fig. D). The flipping of the radial component can be used to validate the low P velocity. We modeled the degree of magma melt by assuming a fluid-filled porous material consisting of granite and a mixture of rhyolite melt and supercritical water and CO₂ at temperature of 800°C and pressure at 5 km. We found that this shallow magma body has a volume of over 4,300 km³ and is at least 32% melt saturated with about 8% water plus CO₂ by volume.

References

Chang, W. L., R. B. Smith, C. Wicks, J. M. Farrell, and C. M. Puskas, Accelerated uplift and magmatic intrusion of the Yellowstone Caldera, 2004 to 2006, *Science*, 318, 952-956, 2007.

Chu, R., D. V. Helmberger, D. Sun, J. M. Jackson, and L. Zhu, Mushy magma beneath Yellowstone, *Geophys. Res. Lett.*, 37, L01306, 2010.

Acknowledgements: All waveform data used in this study were obtained from IRIS Data Management Center. This work is funded by the Tectonics Observatory at California Institute of Technology under Grant No. GPS.TO2-4.1-GRANT.MOORETO2. This is contribution 10035 of the Tectonics Observatory at Caltech.



Recent GPS and InSAR studies show that the Yellowstone caldera is uplifting at a rate of 7 cm/year, which is apparently related to a magma recharge (Chang *et al.* 2007, Fig. A). In receiver functions recorded by EarthScope station H17A from 100 teleseismic earthquakes in 2008, two P-to-SV converted phases exist that are consistent with the top and bottom of a low velocity layer (LVL) at about 5 km depth beneath the Yellowstone caldera (Fig. B and C). Comparisons of synthetic waveforms and observed data for two velocity reductions are shown in Fig. D. Our preferred P- and S-wave velocities suggest at least 32% melt saturated with about 8% water plus CO₂ by volume.

Structure of the Chesapeake Bay Impact Crater from Wide-Angle Seismic Waveform Tomography

W. Ryan Lester (Virginia Tech; now at U. Texas Austin), John A. Hole (Virginia Tech), Rufus D. Catchings (U. S. Geological Survey, Menlo Park), Florian Bleibinhaus (University of Salzburg)

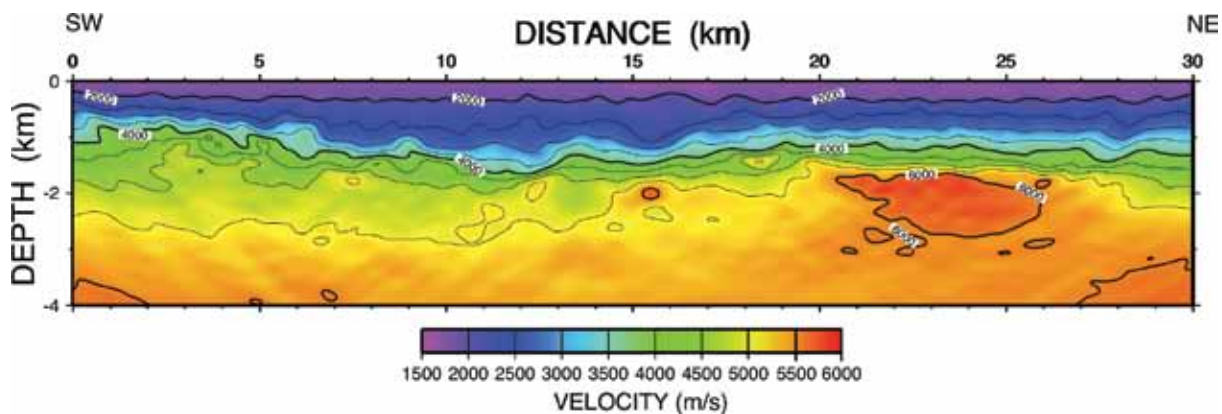
The Chesapeake Bay impact structure is one of the largest and most well preserved impact structures on Earth. It has a unique morphology composed of an inner crater penetrating crystalline basement surrounded by a wider crater in the overlying sediments. In 2004, the U.S. Geological Survey conducted a seismic survey with the goals of constraining crater structure and in support of the drilling of a borehole into the deepest part of the crater [Catchings *et al.*, 2008]. Waveform inversion was applied to these data to produce a higher-resolution velocity model of the crater. Northeast of the crystalline crater, undeformed, eastward-sloping crystalline basement is ~1.5 km deep. The edge of the inner crater is at ~15 km radius and slopes gradually down to a depth of 1.5–1.8 km. A central peak of 4-5 km radius rises to a depth of ~0.8 km. Basement velocity in the crystalline crater is much lower than undeformed basement, which suggests ~10% fracturing of the crater floor, and up to 20% fracturing of the central uplift. A basement uplift and a lateral change of basement velocity occur at a radius of ~11 km, and are interpreted as the edge of the transient crater. Assuming a 22-km diameter transient crater, scaling laws predict a ~30 km diameter crater and central peak diameter of 8-10 km, consistent with the seismic image. This indicates that post-impact collapse processes that created the ~30-km diameter crystalline crater were unaffected by the much weaker rheology of the overlying sediments.

References

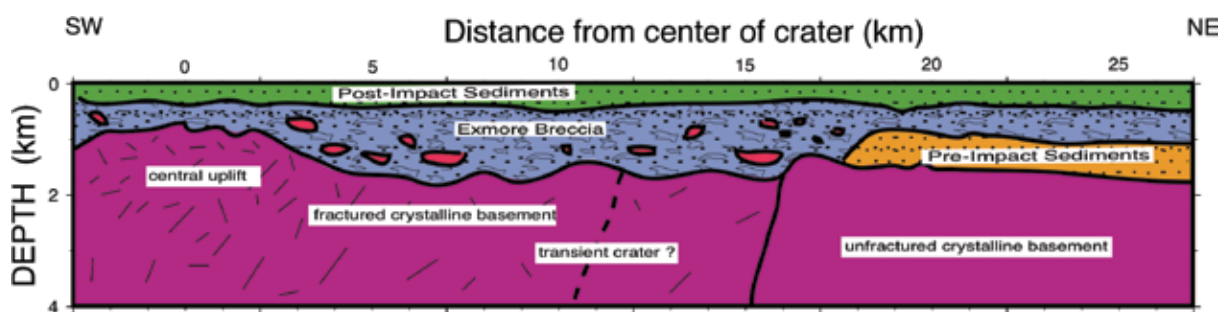
Catchings, R. D., D. S. Powars, G. S. Gohn, J. W. Horton Jr., M. R. Goldman, and J. A. Hole (2008), Anatomy of the Chesapeake Bay impact structure revealed by seismic imaging, Delmarva Peninsula, Virginia, USA, *J. Geophys. Res.*, 113, B08413.

Lester, W. R., (2006), Structure of the Chesapeake Bay Impact Crater from Wide-Angle Seismic Waveform Tomography, M.S. Thesis, Virginia Tech.

Acknowledgements: The data were acquired by the U.S. Geological Survey funded by the National Cooperative Geologic Mapping Program and used IRIS-PASSCAL seismometers.



Seismic velocity model produced by waveform inversion of 3-16 Hz data.



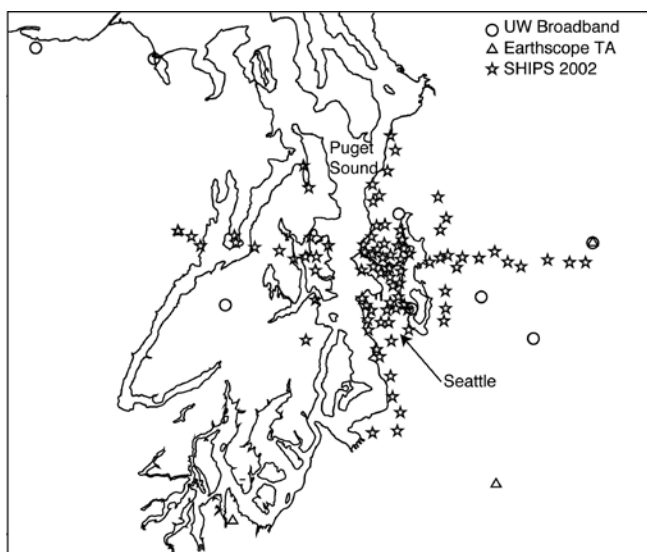
Model of the inner crystalline crater of the Chesapeake Bay impact structure as interpreted from the seismic model. The crater is defined at the base of the Exmore tsunami breccia.

Imaging the Seattle Basin to Improve Seismic Hazard Assessments

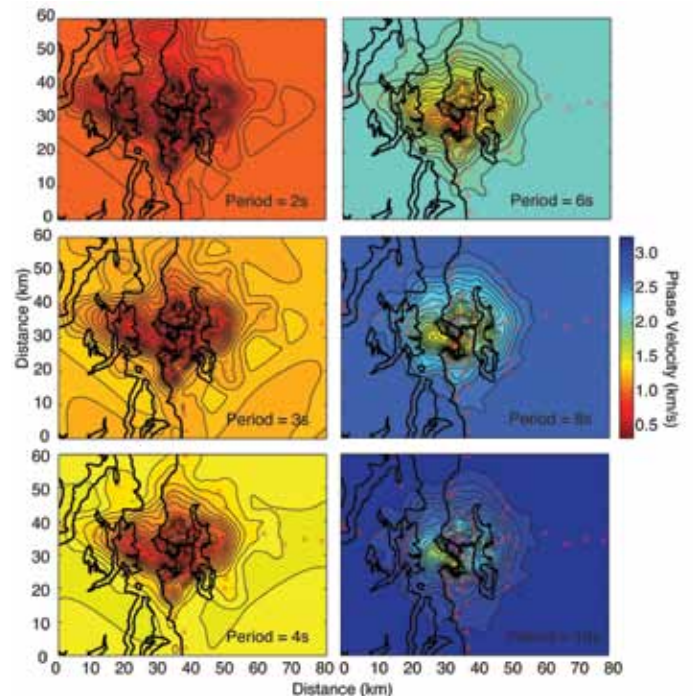
Andrew A Delorey (*University of Washington*), John E Vidale (*University of Washington*)

Much of Seattle lies atop a deep sedimentary basin. The Seattle Basin amplifies and distorts the seismic waves from nearby moderate and large earthquakes in ways that modulate the hazard from earthquakes. Seismic hazard assessments heavily depend upon upper crustal and near-surface S-wave velocity models, which have traditionally been constructed from P-wave models using an empirical relationship between P-wave and S-wave velocity or by interpolating across widely spaced observations of shallow geologic structures. Improving the accuracy and resolution of basin S-wave models is key to improving seismic hazard assessments and predictions for ground shaking. Tomography, with short-period Rayleigh waves extracted using noise interferometry, can refine S-wave velocity models in urban areas with dense arrays of short period and broadband instruments. We apply this technique to the Seattle area to develop a new shallow S-wave model for use in hazard assessment. Continuous data from the Seismic Hazards in Puget Sound (SHIPS) array as well as permanent stations from the Pacific Northwest Seismograph Network (PNSN) and Earthscope's Transportable Array (TA) have inter-station distances as short as a few kilometers. This allows us to extract Rayleigh waves between 2 and 10 seconds period that are sensitive to shallow basin structure. Our results show that shear wave velocities are about 25% lower in some regions in the upper 3 km than previous estimates. Using the new velocity model we run earthquake simulations using a finite difference code to validate the model, and then to make predictions on the level of ground-shaking for various realistic earthquake scenarios at various locations around the urban area.

Acknowledgements: This study is funded by the National Earthquake Hazards Program (NEHRP).



Shown are the stations used for this study. The black curves indicate the coast-line of Puget Sound and Seattle is located where stations are clustered in the center of the figure. The UW Broadband (circles) and Earthscope Transportable Array stations (triangles) were used to get background velocity and the SHIPS stations (stars) were used to image the Seattle Basin.



Shown are Rayleigh wave phase velocities for periods between 2 and 10 seconds.

Earthquake Hazard Class Mapping by Parcel in Las Vegas Valley

John N. Louie (University of Nevada, Reno), Satish Pullammanappallil (Optim SDS), Aasha Pancha (Optim SDS), Travis West (Optim SDS), Werner Hellmer (Clark County Building Department)

Clark County, Nevada is completing the Nation's very first effort to map earthquake hazard class systematically through an entire urban area. The resulting geotechnical shear-velocity map is a layer added to the County's existing soil-hazards map. The map already includes layers such as fault proximity, ground subsidence, and potential for swelling clay soils. The new earthquake-hazard map layer will be available on the County's web GIS interface. Geotechnical shear velocity is a basic building block in foundation design, and in predictions of potential for ground liquefaction, landslides, and seismic shaking, as a few examples. The map will be used in development and disaster response planning, in addition to its direct use for building code implementation and enforcement. Clark County contracted with the Nevada System of Higher Education to apply the refraction microtremor geophysical surveying technique, a State of Nevada-owned technology, to the hazard classification of about 500 square miles Las Vegas Valley.

The parcel map includes almost 9000 measurements that classify parcels on the NEHRP hazard scale, from NEHRP A at least hazardous to NEHRP E at the most. No site in Nevada has yet been measured to be less hazardous than NEHRP B or more hazardous than NEHRP D; and this represents the range of classifications found in unincorporated Clark County. The measured parcel map shows a clearly definable NEHRP B-C boundary on the west side of Las Vegas Valley, rarely more than 300 m wide. The NEHRP C-D boundary is on the other hand much more complex. Using the parcel map in computing shaking in the Valley for scenario earthquakes is crucial for obtaining realistic predictions of ground motions. For Las Vegas the principal earthquake hazard is from the Furnace Creek fault system, capable of M7.5 events. Animations of shaking show the expected strong trapping and long shaking durations within basins, as well as diffusion and scattering of energy between the many basins in the region. Despite affecting only the very shallowest zone of models (<30 m), the Vs30 geotechnical shear-velocity from the parcel map shows clear correlation to 0.3-Hz PGV predictions in basins. Increasing basin thicknesses from 0 to 1.3 km correlate with increased PGV, but the basin effect at 0.3 Hz saturates for basin thicknesses greater than 1.3 km; deeper parts of the basin show variance and uncertainty of a factor of two in predicted PGV.

Acknowledgements: Research supported primarily under contract to the Clark County Building Department; also partially by the U.S. Geological Survey (USGS), Department of the Interior, under USGS award number 08HQGR0015; and by a 2006 Fulbright Senior Scholar award to Louie for work in New Zealand. The views and conclusions contained in this document are those of the authors and should not be interpreted as necessarily representing the official policies, either expressed or implied, of the U.S. Government.

Preliminary hazard map of a portion of Las Vegas Valley, Nevada, prepared from measurements of 1265 sites as of March 2008. (Map book 163 – green numbers – was mapped later that year.) A sharp NEHRP B-C boundary (green to orange) is visible between map books 176 and 177; the NEHRP C-D boundary (orange to red in map book 162) is much more complicated, requiring dense measurements to locate accurately.



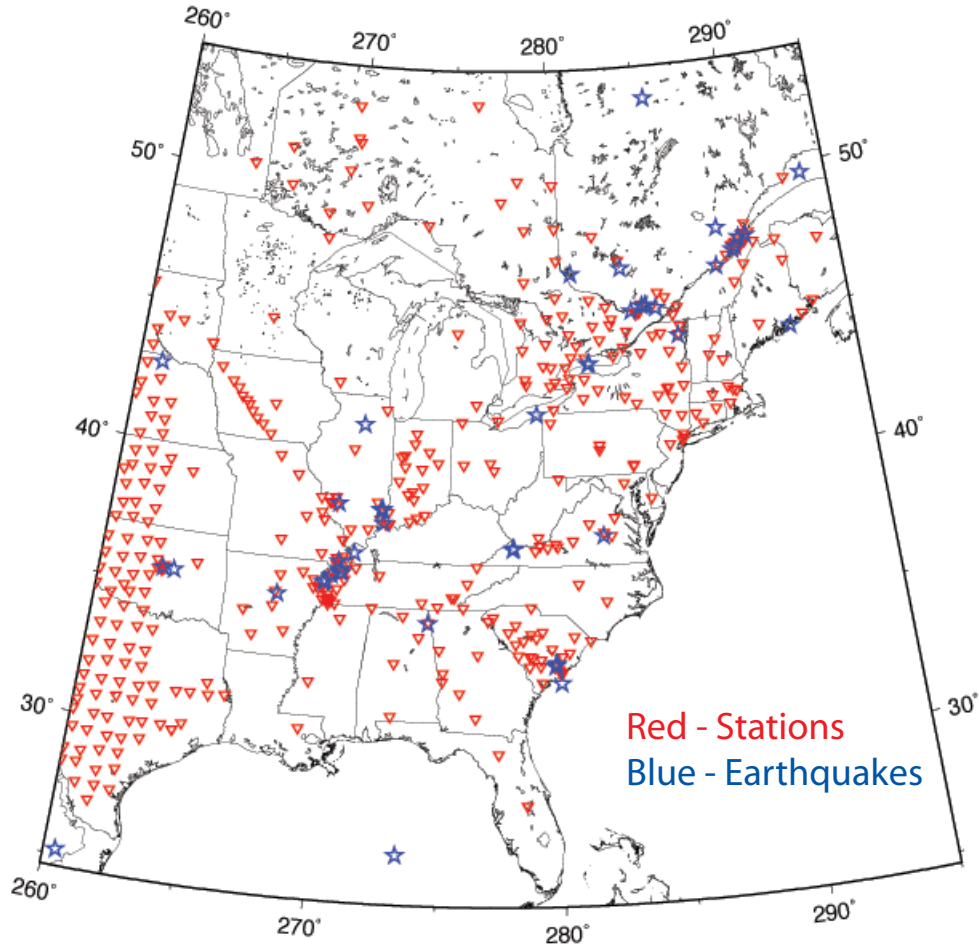
Developing a Database of ENA Ground Motions for NGA East

Chris Cramer (CERI, University of Memphis)

A five-year Next Generation Attenuation (NGA) East project to develop new ground motion prediction equations for stable continental regions (SCRs), including eastern North America (ENA), has begun at the Pacific Earthquake Engineering Research (PEER) Center funded by the Nuclear Regulatory Commission (NRC), the U.S. Geological Survey (USGS), the Electric Power Research Institute (EPRI), and the Department of Energy (DOE). As part of a pre-project effort, the NRC has funded the two-year initial development of an ENA database of ground motions similar to the NGA active-tectonic-regions strong-motion database. This initial effort focused on database design and collection of appropriate $M > 4$ ENA broadband and accelerograph records to populate the database. Ongoing work under PEER funding will focus on adding records from smaller ENA earthquakes and from other SCRs such as Europe, Australia, and India. This effort to develop a database of ENA ground motions for the NGA East project has used waveform data from GSN and USArray stations.

Acknowledgements: This research was supported under USGS cooperative agreement 07CRAG0015 and is currently supported by a contract with PEER.

NGA East Earthquakes and Stations



The stations and earthquakes used in the NGA East project so far.

Seismic Wave Gradiometry Using Multiwavelets: Documented Surface Wave Reflections

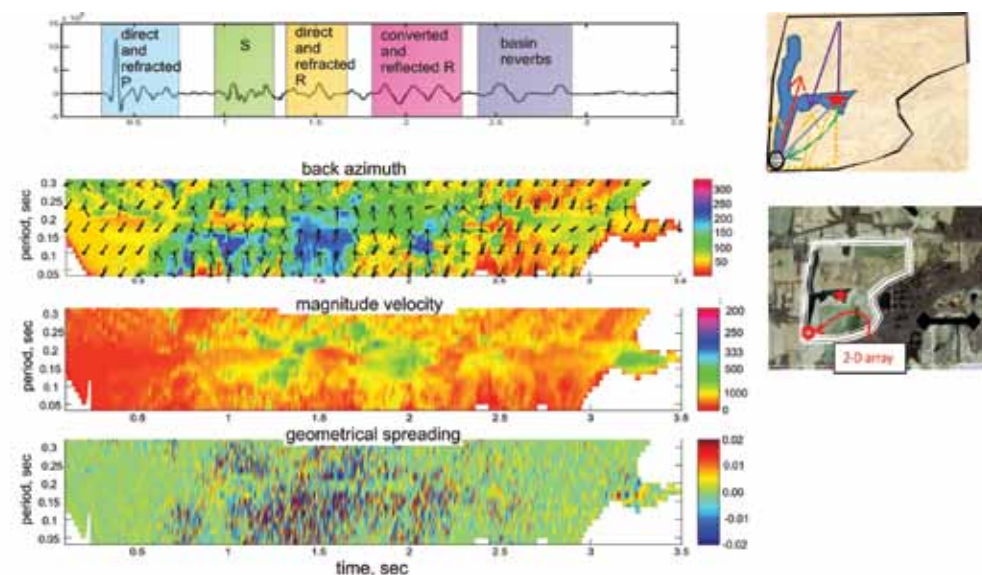
Christian Poppeliers (*Augusta State University, Dept. of Chem. and Physics*)

In the IRIS-produced document “Seismological Grand Challenges in Understanding Earth’s Dynamic Systems”, states several challenges to the seismological community. The work presented here addresses the second Challenge: ‘How Does the Near Surface Environment Affect Natural Hazards and Resources’. Specifically, this work makes strides in quantifying highly complex scattering affects attributed to near-surface geologic conditions using a new seismic processing technique known as seismic wave gradiometry. The method is based on using displacement gradients as measured by a small scale array to estimate wave velocity, wave propagation direction, and spatial amplitude changes at all points on the seismogram [e.g. *Langston, 2007*]. Conventional seismic array processing is not ideally suited to resolve highly complex wave attributes as the wavelength of the wave is typically much smaller than the array aperture. Thus, small-scale time-dependant scattering affects may be missed. Conversely, an array designed as a gradiometer has an aperture of less than 10% of the smallest wavelength of the wavefield being analyzed. Thus a gradiometer is essentially a “point array”, recording the wavefield within a fraction of a wavelength.

The work presented here shows an example of complex surface wave interactions as recorded at the edge of an artificially-created sedimentary basin [Poppeliers, 2010]. The study site consists of a former open-pit coal mine in which the pit has subsequently been backfilled with mine tailings [Poppeliers and Pavlis, 2002]. A series of artificial-source explosions provided the seismic source. Because the wave attributes are highly frequency dependant, we have incorporated multi-wavelets into existing wave gradiometry methodologies, which allows us to quantify frequency-dependent wave attributes as well as calculate formal uncertainty estimates; the result is that wave attributes, as well as their confidence intervals, can be estimated as a function of time and frequency. The figure shows that the estimated vector slowness of the vertical-component wavefield suggests a series of reflected surface waves that traverse the basin multiple times. The reflections of the surface waves likely occur at the vertical boundary between the unconsolidated mine tailings and the surrounding bedrock.

References

- Poppeliers, C., 2010, Seismic Wave Gradiometry Using the Wavelet Transform: Application to the Analysis of Complex Surface Waves Recorded at the Glendora Array, Sullivan, Indiana, USA., *Bull. Seismol. Soc. Amer.*, 100, 1211-1224.
- Poppeliers, C., G.L. Pavlis, 2002, The Seismic Response of a Steep Slope: High-Resolution Observations with a Dense, Three-Component Seismic Array, *Bull. Seismol. Soc. Amer.*, 92, 3102-3115.
- Langston, C.A., Wave Gradiometry in Two Dimensions, *Bull. Seismol. Soc. Amer.*, 97, 401-416.



Multiwavelet seismic wave gradiometry applied to the active-source data collected by a portion of the Glendora array. The seismogram shows the vertical-component displacement. The colored boxes show the wave arrivals interpreted with the help of the resolved wave attributes. The panel showing the resolved back azimuth shows a colormap that corresponds to resolved back azimuth as well as “stick-and-ball” figures as a function of both time and frequency. The ball indicates a given time-frequency location, where the stick points back towards the resolved source. 95% confidence intervals of resolved back azimuth are also shown. The panel showing the magnitude velocity shows a prominent low-velocity arrival between 1.0 and 2.0 seconds which corresponds to various surface wave arrivals. For brevity, formal uncertainties are not shown for the magnitude velocity or geometrical spreading estimates.